Tumor necrosis factor induces cholesterol accumulation in human arterial endothelial cells through LDL receptor surface redistribution

Emmanuel Ugochukwu Okoro

Department of Microbiology, Immunology, and Physiology, Meharry Medical College, Nashville, TN 37208

Correspondence: Emmanuel U. Okoro
E-mail: eokoro@mmc.edu

Running title: TNFα on arterial endothelial LDL uptake

Keywords: cell surface receptor, cholesterol, endothelial cell, lipoprotein, low-density lipoprotein (LDL), tumor necrosis factor (TNF)

ABSTRACT

Tumor necrosis factor alpha (TNFα) and low density lipoprotein (LDL) are important modulators of the atherosclerotic process. Here, the effect of TNFα on confluent primary human aortic endothelial cell (pHAEC) LDL-derived lipids and trafficking were investigated. TNFα promoted up to 2 folds increase in cellular cholesterol and could induce a massive increase in the non-hydrolysable tracer, Dil, by over 200 folds. The lipid increase was associated with increased ^{125}I-LDL surface binding. Further, Dil-LDL cellular association was blocked by excess unlabeled LDL, but not oxidized LDL (oxLDL). Moreover, TNFα-induced Dil and cholesterol increase were enhanced by the endosomal pH-raising agent, chloroquine. Internalization of Dil-LDL was reduced by the scavenger receptor B1 (SR-B1) antagonist, BLT-1, and the LDLR family antagonist, proprotein convertase subtilisin/kexin type 9 (PCSK9), but not receptor associated protein (RAP). Additionally, surface accessible LDLR was higher in TNFα-treated cells by about 30 folds, without a significant change in total LDLR. Correspondingly, specific LDLR antibody blocked Dil-LDL internalization to undetectable levels, and Dil-apoE3-VLDL by 94%, but had no effect on Dil-HDL3 internalization. TNFα did not increase Dil-HDL3 cellular association. Further, ACAT inhibitor reduced cholesteryl esters, but not the total cholesterol increase induced by TNFα. On pHAECs grown on transwell inserts, TNFα did not enhance apical (AP) to basolateral (BL) LDL cholesterol or Dil release. It is concluded that TNFα induces LDLR surface localization and that LDLR does not promote AP to BL LDL transport across pHAECs.

INTRODUCTION

TNFα was originally discovered as a tumor-selective hemorrhagic factor (1,2). However, it is now recognized to have multiple cell-type dependent effects (3,4). Released as a 17 kD soluble protein from a transmembrane precursor by tumor necrosis factor converting enzyme (TACE) (5-7), this cytokine mainly promotes changes that facilitate leukocyte (inflammatory) functions. (4,8). Acting through the rapid-acting transcription factor, nuclear factor kappa B (NF-kB), it can induce expression of pro-inflammatory mediators such as interleukin 1 and 2 (9,10). Likewise, it is capable of inducing apoptosis (11-13), possibly through c-jun N-terminal kinase (JNK) activation (14-16). Thus TNFα may clear way for passage of leukocytes through target epithelial cell apoptosis. On the

other hand, it can induce proliferation of lymphocytes and fibroblasts (12,17-19). This ability to induce proliferation have been reported to be due to upregulation of growth factor receptors (20,21) or growth factor release, such as vascular endothelial growth factor (VEGF) (21-23) .

Some report that TNFα is atherogenic (24-26). The pro-atherogenic arm of TNFα is in part due to its ability to enhance monocyte entry into the intima through induction of adhesion molecules on arterial endothelial cells. In atherosclerotic lesions, macrophages (27) and smooth muscle cells (27,28) have been reported to express TNFα, where it acts on overlying endothelial cells to stimulate expression of leukocyte adhesion molecules such as E-selectin, vascular cell adhesion molecule-1 (VCAM-1), and intercellular adhesion molecule-1 (ICAM-1) (29,30). More, it induces expression of monocyte chemoattractant protein I (MCP-1) (31), which stimulates gradient migration of lymphocytes and monocytes (32,33).

Still, TNFα can have a neutral or ambiguous effect on atherosclerosis development (34,35). For example, targeted elimination of tumor necrosis factor receptor (TNFR) have produced mixed results. TNFR1 has been reported to be anti-atherogenic (34,36), pro-atherogenic (24,37,38), or neutral (39). Likewise, TNFR2 has been reported to be pro-atherogenic (40) or neutral (34). These conflicting results suggest that the mechanisms by which TNFα affects atherosclerosis development need further clarification. Of note, TNFα deletion is associated with elevated HDL cholesterol, but reduced LDL cholesterol, indicating that it regulates serum lipoprotein levels (25).

Background inflammation is an independent risk factor for atherosclerotic cardiovascular disease (41). Serum concentration of TNFα increases with severity of atherosclerotic lesion (42,43) and age (44). Thus, it has been reported to be about 200 folds higher in the atherosclerotic lesion than in the circulating blood (45).

Although TNFα levels in the arterial wall are elevated in the late stages of atherosclerosis, this elevation need not occur late in the disease. Elevated native LDL, which is pro-atherogenic, (46,47), stimulates TNFα production in smooth muscle cells (48). Further, viremia, bacteria, and other forms of microbial infections affecting the artery may lead to focal elevation of TNFα, which can initiate atherosclerosis development (49). Certain endothelial dysfunctions, such as impaired NO release, are well-characterized in late atherosclerotic lesions (50). However, other endothelial functions that may affect initiation and progression of atherosclerosis are not well known.

Unlike macrophages (51,52) and smooth muscle cells (51,53), normal confluent endothelial cells are resistant to cholesterol accumulation (54). However, fibro-fatty atherosclerotic lesions contain endothelial foam cells with intact monolayer (55-57). In this report, I present evidence of non-inflammatory function of TNFα. It will be shown that TNFα increases pHAEC cholesterol and lipid accumulation through increased surface accessible low density lipoprotein receptor (LDLR).

RESULTS

TNFα enhances cholesterol accumulation and LDL binding to pHAECs. Atherosclerotic lesion is characterized by release of inflammatory cytokines, among which is TNFα. To evaluate the effect of TNFα on pHAECs cholesterol content, confluent pHAECs were treated with or without TNFα and the cellular cholesterol content was measured. As is shown in **Figure 1A,** TNFα significantly increased unesterified cholesterol, and to a greater degree, esterified cholesterol (**Figure 1B**). **Figure 1A-B** also show that the ability of TNFα to induce cholesterol accumulation plateaus at around 100 µg/ml LDL protein. To evaluate whether TNFα

affects the ability of LDL to bind to the cells, ^{125}I-LDL binding was performed. **Figure 1C** shows that TNFα enhanced ^{125}I-LDL surface releasable ^{125}I-LDL at 4 °C, after the cells were pre-treated at 37 °C. The amount released increased in the presence of 20 folds unlabeled LDL. This indicates that the ^{125}I-LDL bound to some native LDL receptor. Further, cell-associated ^{125}I-LDL was also higher on TNFα-treated pHAECs (**Figure 1D**), indicating higher ^{125}I-LDL internalization.

LDL oxidation is not required for TNFα-induced LDL binding and internalization. Having demonstrated that TNFa promoted LDL binding to pHAECs (Figure 1), the requirement for oxidative modification of LDL was investigated. Particularly, TNFα has been reported to promote release of the reactive oxygen species, superoxide and hydrogen peroxide (58,59). Hence, experiments were performed to determine whether oxidative modification of LDL is a prerequisite to TNFα-induced LDL binding. To visualize TNFα-induced LDL binding and subsequent internalization, Dil-LDL was used.

As can be seen in **Figure 2A**, Dil accumulation within the pHAECs can be seen as intracellular clusters located primarily to either pole of the cell. This internalized Dil-LDL was significantly increased through TNFα pre-treatment (**Figure 2A-B**). It can also be seen in **Figure 2A-B** that excess unlabeled native LDL blocked binding and internalization of Dil-LDL to undetectable levels. This demonstrates that native LDL components, and therefore receptors, are required for Dil-LDL binding and internalization. Excess unlabeled oxLDL, on the other hand, had weaker effect on Dil-LDL association in control cells. It had no effect on TNFα-treated cells (**Figure 2B**). The weak suppression of Dil-LDL association under control conditions is not too surprising. It can be seen in **Figure 2C** that oxLDL retains some apoB moiety, which can explain the residual effect on Dil-LDL association.

TNFα induces massive Dil over [^{3}H]CE lipid accumulation from LDL. The lipids, Dil and ^{3}H-cholesteryl esters ([^{3}H]CE), are stably fixed within LDL. To evaluate the ability of pHAECs to retain LDL hydrolysable [^{3}H]CE or the non-hydrolysable Dil, the cells were treated with increasing concentration of TNFα in the presence of [^{3}H]CE-LDL or Dil-LDL. As is shown in **Figure 3A**, ^{3}H-cholesterol accumulation induced by [^{3}H]CE-LDL and increasing TNFα plateaued at about 30 ng/ml TNFα, increasing to about 2 folds. On the other hand, Dil accumulation increased by about 50 folds (**Figure 3B**). Next, cells were treated with increasing Dil-LDL concentration without (**Figure 3C**) or with TNFα (**Figure 3D**). As is shown in **Figure 3C**, 400 μg/ml Dil-LDL increased intracellular Dil level by about 50 folds compared to that at 1 μg/ml under control condition. Compared to Ctrl at 400 μg/ml Dil-LDL, TNFα increased the intracellular Dil by over 200 folds (**Figure 3D**).

Blockage of endosomal acidification enhances TNFα-induced LDL lipid accumulation. The lowering of pH facilitates disintegration and degradation of internalized LDL through the lysosomal compartment. This degradation is suppressed by the pH-raising compound, chloroquine (60). To evaluate whether a similar phenomenon occurs in pHAECs, the cells were treated in the presence or absence of chloroquine. The presence of chloroquine caused the Dil to accumulate circumferentially within the cells, presumably in defective lysosomal structures (**Figure 4A**). As can be seen in **Figure 4A-B**, chloroquine greatly enhanced Dil accumulation without TNFα. The presence of TNFα further increased the amount of chloroquine-induced cellular Dil. Chloroquine also increased ^{3}H-cholesterol level from [^{3}H]CE-LDL. However, it was not as pronounced as in the case of Dil (**Figure 4C**).

Effect of native lipoprotein receptors on Dil-LDL cell association in pHAECs and

hepatocytes. Having found evidence that TNFα promotes cholesterol accumulation in pHAECs through enhanced endocytosis of native LDL, I next investigated what members of the LDLR family are responsible, in addition to the potential role of SR-B1. Specifically, LDL-derived lipid accumulation have been shown to be increased by SR-B1(61-63). To investigate these possibilities, experiments were performed with their respective inhibitors. The data in **Figure 5A-B** show that blockage of SR-B1 selective uptake with BLT-1 reduced TNFα-induced Dil-LDL internalization. Likewise, the pan-LDLR family blocker PCSK9 (64-66), but not RAP (67), suppressed the Dil accumulation.

SR-B1 and the LDLR family members are abundantly expressed in hepatocytes. Thus, to evaluate whether RAP activity is measurable in hepatocytes, the cells were treated with all the inhibitors (**Figure 5C**). The results show that the failure of RAP to inhibit Dil-LDL internalization is specific to pHAECs. Since RAP has been reported to be ineffective against LDLR (68), the data point to LDLR as the most likely candidate.

TNFα increases surface-accessible LDLR without a significant change in total protein. Having pinpointed LDLR as a likely receptor through which TNFα induces cholesterol and Dil accumulation in pHAECs, I next evaluated the effect of TNFα on the LDLR protein product (**Figure 6A-B**). The data show that TNFα did not significantly increase total LDLR. However, it greatly promoted association of surface LDLR to its antibody in the culture medium as demonstrated by enhanced upward shift of the LDLR protein (**Figure 6A**).

LDLR mediates TNFα-induced LDL internalization. Up to now, the data suggest that SR-B1 and/or LDLR contributes to the mechanism by which TNFα induces Dil-LDL binding and internalization. To evaluate the roles of these receptors, experiments were performed to test SR-B1 surface expression with Dil-HDL3 (61,63) and LDLR surface expression with Dil-LDL and Dil-apoE3-VLDL. Since lipid-bound apoE binds all the LDLR family members (69), information about the type of family member involved can further be evaluated in the presence of specific LDLR antibody. Accordingly, the data in **Figure 7A-B** show that Dil-HDL3 internalization in pHAECs was not enhanced by TNFα. Further, LDLR antibody did not block Dil-HDL3 cellular association. In contrast, LDLR antibody blocked TNFα-induced Dil-LDL cell association to undetectable levels (**Figure 7C-D**) and blocked TNFα-induced Dil-apoE3-VLDL association by approximately 94% (**Figure 7E-F**). The overall data thus demonstrate that LDLR is the dominant receptor for uptake of non-HDL lipoproteins in pHAECs, with or without TNFα.

TNFα induces surface redistribution of LDLR. The data presented in Figure 6 indicated that more surface LDLR are induced by TNFα. Having found that LDLR mediates TNFα-induced LDL internalization without a significant change in the total protein (Figure 6), I investigated the extent of surface LDLR differences through immune-fluorescent microscopy. As can be seen in **Figure 8A**, TNFα did not enhance association of control antibody with the cells, but significantly induced association with specific LDLR antibody by 30 minutes at 37 °C. This indicates that TNFα did not promote non-selective endocytic processes. The surface distribution of LDLR (arrows) and the internalization of the surface LDLR (arrow heads) in cells treated with TNFα can be seen in **Figure 8B**.

The total amount of surface LDLR bound by the antibody at 37 °C can be seen to increase with time. At 0, 5, 30, and 120 minutes, there was about 30, 50, 7, and 2 folds, respectively, more surface LDLR in TNFα-treated cells compared to control cells at the corresponding time (**Figure 8C-D**). This demonstrates that LDLR antibody rapidly binds surface LDLR in the case of TNFα-treated cells, plateauing by about 2

hours. This plateauing is consistent with the finding that the total LDLR is not significantly different between control and TNFα-treated pHAECs (Figure 6).

ACAT inhibitor does not prevent TNFα-induced LDL cholesterol accumulation. It has been reported that TNFα induces cholesteryl ester accumulation in monocytes through enhanced ACAT activity in the presence of oxLDL (70). To evaluate the extent to which enhanced ACAT activity is responsible in raising pHAEC cholesterol in the presence of LDL, the cells were with or without ACAT inhibitor, Sandoz 58-035. As is reported in **Figure 9A-B**, inhibition of ACAT activity slightly raised the unesterified cholesterol, and significantly suppressed cholesteryl ester accumulation. Despite this inhibition, the TNFα-induced total cholesterol accumulation, now mainly in the unesterified form, was not prevented (**Figure 9A,C**). ACAT inhibition also reduced the total cholesterol in the cells, with or without TNFα stimulation (**Figure 9C**). This is a known effect of ACAT inhibition. The higher elevated unesterified cholesterol is more likely to be effluxed from the cells than the esterified one (71).

TNFα does not affect AP to BL release of degraded LDL protein. To address the effect of increased LDLR-mediated uptake of LDL on apical to basolateral LDL protein transport, the pHAECs were grown to confluence on transwell inserts, as shown in **Figure 10A**. ^{125}I-LDL detected in the BL medium was either non-intact (**Figure 10B**) or intact (**Figure 10C**). In **Figure 10B**, it is shown that unlabeled LDL competitor reduced the amount of non-intact ^{125}I-LDL in a TNFα-independent manner. In contrast, the unlabeled competitor had no effect on the intact ^{125}I-LDL measured in the BL medium (**Figure 10C**). The overall data thus indicate that the LDLR cargo is not efficiently trafficked in a polarized manner in pHAECs.

TNFα does not affect AP to BL LDL lipid release. To determine whether LDLR facilitates AP to BL LDL lipid transport, the pHAECs on transwell inserts were incubated with LDL colabeled with Dil and ^{3}H-cholesteryl esters (**Figure 11A-B**). As can be seen in the figures, TNFα dose-dependently increased the accumulation of Dil-LDL on the pHAECs grown on transwell inserts, in the same manner as those grown on plastic dishes. Similar to pHAECs on plastic dishes, LDLR antibody significantly blocked uptake of Dil-LDL by pHAECs grown on transwell inserts. The corresponding uptake of ^{3}H-cholesteryl esters is shown in **Figure 11C**. The ^{3}H-cholesteryl ester accumulation induced by TNFα is blocked in the presence of antibody against LDLR. Surprisingly, LDLR blockage had no effect on the amount of measurable ^{3}H-choleseryl ester detectable in the BL medium (**Figure 11D**). This is consistent with the BL Dil-LDL, whose value was independent of TNFα treatment (**Figure 11E**).

DISCUSSION

Native LDL modification due to oxidation (72,73), aggregation (74), or complex formation with proteoglycans (75-77) is known to promote cholesterol accumulation in macrophages. Although confluent arterial endothelial cells are resistant to cholesterol accumulation induced by lipoproteins, my results demonstrated that this can be altered in the presence of TNFα. Thus, LDL modification is not an absolute requirement for LDL-induced cholesterol or lipid accumulation. The data suggest that pHAECs, like macrophages, may be susceptible to changes related to excess cholesterol loading, including apoptosis, which is known to occur in the most advanced form of atherosclerotic lesions (78).

Interestingly, bovine brain microvascular endothethial cells have been reported to promote apical to basolateral transport of LDL through LDLR (79). It thus appears that LDLR trafficking in brain microvascular endothelial cells is different from human aortic endothelial

cells. Additionally, it has been reported that AP to BL LDL transport occurs in vivo across arterial endothelial cells (80). My findings suggest that this transport is probably not through LDLR. SR-BI, on the other hand, have been reported to bind LDL (61,81,82). Since SR-B1 have been shown to cause AP to BL transport of HDL in bovine aortic endothelial cells (83), it is possible that it can do the same for LDL in human aortic endothelial cells. However, the results indicate that LDLR is the dominant receptor utilized by pHAECs for LDL uptake. The binding of LDLR to RAP is controversial. On one hand, it has been reported to bind LDLR (84), while others report the opposite (68). My data suggest that if it binds LDLR, it does not interfere with the ability of LDLR to subsequently internalize LDL.

TNFα is a pleiotropic autocrine and paracrine mediator important in multiple signaling cascades that range from activating immune cells to fight viruses, bacteria, and cancer cells, to promoting entry of monocytes and lymphocytes into atherosclerotic lesions (85-87). The latter process is recognized to be pro-atherogenic. TNFα has also been reported to play an important role in the current COVID-19 pandemic (88). Thus, nonspecific disruption of TNFα activity in the animal interferes with many important biological functions (89). My finding that TNFα upregulates surface LDLR function in pHAECs implies that it is possible to regulate this process selectively, while leaving the beneficial functions of TNFα intact. Excess cholesteryl ester accumulation in arterial endothelial cells is likely to lead to endothelial dysfunction due, in part, to space disruption.

Native lipoproteins that are potentially atherogenic exist in the form of LDL and β-VLDL. Unlike normal VLDL which contains triglycerides and apoB as their major constituents, β-VLDL is enriched in apoE and cholesterol (90). β-VLDL levels increase as the plasma cholesterol values increase in animals fed high cholesterol diet (91). My finding that apoE-enriched Dil-VLDL produced a marked increase in Dil accumulation, further enhanced by TNFα, suggest that it can initiate endothelial dysfunction in an LDLR-dependent manner. In addition to carrying cholesterol and cholesteryl esters as its primary cargo, LDL may transport other lipid soluble agents. Thus lipid-soluble drugs carried by non-HDL lipoproteins are predicted to negatively impact endothelial cells in the setting of infections, chronic inflammatory stress, and atherosclerosis.

The significantly greater Dil accumulation over cholesterol indicates that pHAECs have an efficient mechanism of overcoming enhanced LDL uptake. Neutral cholesteryl ester hydrolase activity and endosomal recycling are known to be intact in the presence of chloroquine (63,92). My data suggest that LDL-derived [^{3}H]CE may be hydrolysed outside the lysosome in pHAECs. This type of hydrolysis is typical of HDL cholesteryl ester hydrolysis (63). Another possible explanation behind the higher Dil accumulation may be due to greater free cholesterol efflux induced by TNFα. Thus, it has been reported that TNFα enhances cholesterol efflux (78) and ABCA1 mRNA and protein through NF-kB signaling (93).

It has been reported that TNFα enhances ACAT1 activity in leukocytic cells and promotes cholesteryl ester accumulation in the presence of oxLDL (70). This was not observed in the non-leukocytic cells tested (70). Enhanced cholesterol esterification as the primary mechanism underlying TNFα-induced cholesterol accumulation in pHAECs was not observed in this study. Of note, TNFα and oxidative stress are known to upregulate the oxLDL receptor, lectin-like oxLDL receptor (LOX-1) in arterial endothelial cells (94,95). Elevated cholesterol loading may secondarily elevate ACAT activity (96). The extent to which the mechanism contributed to the findings is unclear.

EXPERIMENTAL PROCEDURES

Materials. Agilent Technologies (Santa Clara, CA): Bond elut column, 12256060. Alfa Aesar (Haverhill, MA*):* 1,10-phenanthroline (PhenA, A16254), tetramethylthiourea (TMTU, L13392). ATCC (Manassas, VA*):* pHAECs (PCS-100-011), vascular basal medium (VBM, PCS-100-030), and vascular endothelial growth factor kit (VEGF, PCS-100-041). BioIVT (Westbury, NY). Caymen Chemical (Ann Arbor, MI*)*: PCSK9 (20631). Cellvis (Mountain View, CA): 96-well glass bottom dishes (P96-0-N). Enzo Life Sciences (Farmingdale, NY*):* Latrunculin A (BML-T119), receptor associated protein (RAP, BML-SE552-0100). Images were obtained using Keyence (Itasca, IL) phase-contrast fluorescence microscope. Pall Corporation (Port Washington, NY): Centrifugal filter (MAP003C36). Perkin Elmer (Waltham, MA): [1,2-3H(N)]-Cholesterol (NET139001). ProSci Inc (Poway, CA): Tumor necrosis factor alpha (TNFα, 96-734). R&D Systems (Minneapolis, MN): anti-goat (NL001), fetal bovine serum (FBS, S11550), LDLR antibody (AF2148), normal goat IgG (AB-108-C). Sigma-Aldrich (St. Louis, MO): BLT-1 (373210), Dil (468495), fatty acid free bovine serum albumin (FAF-BSA, A8806), modified Hanks balanced salt solution (mHBSS, H8264), phosphatase inhibitor (P0044), protease inhibitor (P8340), Sandoz 58-035 (S9318). Spectrum Labs (Cincinnati, OH): Dialysis membrane, 131204. Thermo Fisher Scientific (Waltham, MA): Antibiotic-antimycotic (15240112), desalting columns (89890), iodination beads (28665).

Cell culture and incubations. pHAECs (passages 3-7) were maintained in VBM with growth factor kit (VEGF), ATCC, in the presence of 15% FBS, and antibiotic, antimycotic (100 units/mL of penicillin, 100 µg/mL of streptomycin, and 0.25 µg/mL of amphotericin B, from Thermofisher). Under serum-free conditions, the cells were cultured in VBM, VEGF, with the latter antimicrobials and 0.1% FAF-BSA. Incubations were at 37 °C, unless indicated otherwise. Experiments were best started with pHAECs confluent for 5 days or longer. Separate cells from individuals (2-36 years old) were used during the course of the experiments, with similar results. Overnight incubations in serum medium were 24 ± 5 hours. For cell-associated studies at 37 ºC, cells were washed 3X with mHBSS at 0 ºC. Imaging studies demonstrated that the vast majority of dil-lipoproteins were within the cell under these conditions. For intracellular LDL levels, pHAECs were incubated at 0 °C for 5 minutes with ice cold 400 units/ml sodium heparin in mHBSS, washed twice with the same buffer, then two more times with ice cold mHBSS, to remove surface LDL. Lipids were extracted as described below or the cells were fixed with 4% paraformaldehyde in PBS prior to microscopy.

Lipoprotein purification. All procedures were performed between 0 and 4 °C. Centrifugations and dialysis were performed at 4 °C. Lipoproteins were isolated from freshly drawn human blood anticoagulated with Na_2EDTA (BioIVT). The blood was centrifuged at 4,000 g for 30 minutes to obtain the plasma. To the plasma, butylated hydroxytoluene (BHT) in DMSO was added to 45 µM (0.01%). Then, sequential density ultracentrifugations (97) were performed to obtain d<1.006 (VLDL), d=1.019-1.063 (LDL), or d=1.12-1.21 (HDL3) g/ml. Ultracentrifugations were done using type Ti70 rotor at 50,000 rpm for 20 (VLDL and LDL) or 48 hours (HDL3). The lipoproteins were dialyzed through ~4 kD molecular weight cut-off membrane in 3 successions against ~180 times dialysis buffer (DB): 10 mM Tris-HCl, 150 mM NaCl, 0.3 mM Na_2EDTA, pH 7.5, with deionized water, in the dark, each lasting about 24 hours. After concentration using 3 kD MWCO centrifugal filters, the LDL was filtered through 0.2 µm membrane under sterile conditions. Lipoprotein contents were routinely verified by western blotting and coomassie staining. In addition, the cholesterol and cholesteryl ester contents were verified to be consistent with previous publications (98-100). Lipoprotein concentrations represent the protein content throughout the manuscript.

Cellular cholesterol determination. Lipids were extracted with hexane: isopropanol (1:1) at room temperature for 3 hours, then the solvent was evaporated at room temperature using centrivap concentrator (Labconco). The extracted lipids were redissolved in isopropanol. To determine the unesterified cholesterol content, the lipids in isopropanol were mixed with 10 times volumes of cholesterol assay buffer (CAB): 0.1% fatty acid free BSA (Sigma), 2 mM sodium taurocholate (Beantown Chemical), 50 mM Tris-HCl, pH 7.5, 0.3 mM Na_2EDTA, 5% isopropanol, and 250 mM sucrose, with freshly added 0.5 U/ml horseradish peroxidase (Thermofisher) and 0.02 U/ml cholesterol oxidase (Sigma) in the presence of 30-50 µM scopoletin (101) (excitation 360, emission 460). The CAB was kept at room temperature to ensure full solubilization of the lipids. (Due to the presence of organic solvents, it is recommended that N95 mask be worn). This enzymatic approach is a modification of a previously published procedure (102). Total cholesterol was determined as above, with the addition of 0.1 U/ml cholesteryl esterase (MP Biologicals). Readings were obtained after incubation at 37 °C for 20 minutes. Cholesteryl esters were determined by subtracting unesterified cholesterol from the total cholesterol. The residual cell matter after lipid extraction was lysed with 0.1 M NaOH, 0.1% SDS, for protein reading using BCA assay kit (Thermofisher).

^{3}H-cholesteryl ester ([^{3}H]CE) generation. 40 µCi of ^{3}H-cholesterol (Perkin Elmer) in ethanol was added in 10 µl aliquots to 40 ml of 0.2 µm filtered human serum under sterile conditions. The mixture was incubated at 37 °C for 48 hours in the dark. ^{3}H-cholesteryl esters and other lipids were extracted with chloroform: methanol (103). After evaporation of the solvent, the residue was dissolved in a minimal volume of chloroform. Subsequently, ^{3}H-cholesteryl esters were purified using serial bond elut columns (Agilent Technologies) with several hexane passages, as previously described (104).

Western blotting. pHAECs were lysed with lysis buffer (0.2 % SDS, 2% Triton X-100, PBS, pH 7.5, 2% protease inhibitor and 2% phosphatase inhibitor, Sigma) by sonication at 2 setting (Fisher sonic dismembrator model 100) on ice for 10 seconds. After centrifugation at 16,000 g x 10 minutes at 4 °C, equal volume of loading buffer (8 M urea, 2% SDS, 125 mM Tris-HCl, pH 7.0, 5% glycerol, 10% beta-mercaptoethanol, 0.06% bromphenol blue) was mixed with the supernatant at room temperature. This was followed by electrophoresis, electrical transfer to PVDF membrane, and immunoblotting.

Dil- and/or [^{3}H]CE-Lipoproteins. Generation of Dil-labeled lipoproteins was obtained essentially as previously described (105), with minor modifications. In brief, a mixture of about 2 mg HDL3, LDL, or VLDL protein and 7 ml of human lipoprotein deficient serum was mixed with ~1 mg [^{3}H]CE and/or 0.5 mg Dil in 10 µl DMSO aliquots under sterile conditions. In the case of VLDL, 100 µg apoE3 was included to obtain Dil-apoE3-VLDL. After covering with foil, the mixture was incubated at 37 °C for 21 hours. The lipoproteins were repurified as described above, after adjusting to their respective densities with solid KBr. Combined Dil, [^{3}H]CE-LDL radioactivity was 8.1 dpm/µg protein.

LDL iodination with Na^{125}I. About 2 mg LDL protein in PBS and 10 iodination beads (Thermofisher) were incubated with Na^{125}I for 10 minutes at room temperature in glass vials. The transformation was stopped with 50 mM each of unlabeled sodium iodide and sulfite, and 100 µM BHT in DMSO (0.01%). The labeled LDL was washed with desalting columns, then passed through centrifugal filters, 3 kD MWCO, against dialysis buffer.

^{125}I-LDL cell surface binding. Confluent pHAECs on plastic dishes were cultured with 0 or 5 ng/ml TNFα in 15% serum for 48 hours. Treatment continued with serum-free medium in the continued presence of TNFα for 3 hours to deplete surface-bound LDL. Subsequently, ^{125}I-LDL was added to 15 µg/ml for 1 hour at 37 °C. The cells were then washed two times with PBS at room temperature, then chilled on ice. Afterwards, serum-free medium at 4 °C with 0 (buffer) or 300 µg/ml LDL was added. Following additional incubation at 4 °C for 1 hour, the radioactivity released to the medium was taken as surface-releasable ^{125}I-LDL.

LDL oxidation. LDL was dialysed against PBS at 4 °C, passed through 0.2 µm filter, and incubated at 37 °C for 22 hours with 5 µM $CuSO_4$ in PBS under sterile conditions. After adding BHT in DMSO (0.005%) to 1 µM and Na_2EDTA to 10 mM, the mixture was dialysed against dialysis buffer, and finally filtered through 0.2 µm membrane under sterile conditions.

Dextran-Mn separation of intact and non-intact ^{125}I-LDL. Intact ^{125}I-LDL was separated from non-intact LDL using dextran sulfate, Mn^{2+} procedure essentially as previously described (106). To the BL medium, d<1.21 g/ml FBS was added to 15% to produce a visible precipitate, mixed, then dextran sulfate and MnCl were added to 65 mg/ml and 0.2 M, respectively. After incubation for 20 minutes at room temperature, the mixtures were centrifuged at 5000 g x 5 minutes at 4 °C. The pellet was redissolved with 20 mg/ml dextran sulfate before scintillation counting.

Surface LDLR Detection. Confluent pHAECs in serum medium were incubated with 0 or 100 ng/ml TNFα for 20-24 hours. Subsequently, the media were replaced with serum-free medium containing 10 µg/ml normal goat IgG or LDLR Ab (R&D Systems) in the continued presence of 0 or 100 ng/ml TNFα for 0, 5, 30, or 120 minutes at 37 ºC. Afterwards, the cells were chilled on ice and further incubated at 4 ºC for 1 hour. Then the cells were washed 2X with ice-cold mHBSS, fixed with ice-cold methanol at -20 ºC for 10 minutes, washed once with mHBSS at room temperature, then blocked with 50% human serum in mHBSS, 0.1% sodium azide (blocking buffer) for 1 hour at room temperature. Afterwards, it was replaced with 4 µg/ml red antigoat antibody (R&D Systems) in blocking buffer. Following 30 minute incubation at room temperature, the medium was replaced with mHBSS, washed 3X with blocking buffer (10 minutes each at room temperature), fixed with 4% paraformaldehyde in PBS, followed by fluorescence microscopy.

Fluorescence Microscopy. Fluorescence microscopy was performed using Keyence phase-contrast fluorescence microscope. Images were analyzed using CellProfiler (107). Confocal microscopy was performed using glass bottom dishes (Cellvis).

STATISTICAL ANALYSIS. Data are reported as averages ± standard deviation, where indicated. Analysis of variance, followed by Tukey post hoc testing was done by using statpages.info website.

DATA AVAILABILITY. All data are contained in the manuscript.

ACKNOWLEDGMENTS. The author thanks the Meharry core facility staff for assistance in the using the equipment.

FUNDING

This work was supported through the following grants: Meharry Clinical and Translation Research Center (MeTRC) 5U54MD007593-09 (EUO, Samuel Adunyah), RCMI 5U54MD007586-33 (EUO, Samuel Adunyah), SC1HL101431(Hong Yang). Confocal microscopy core was supported through NIH grants MHD007586 and S10RR025497. The content is solely the responsibility of the author

and does not necessarily represent the official views of the National Institutes of Health.

CONFLICT OF INTEREST

The author declares that he has no conflicts of interest with the contents of this article

REFERENCES

1. Carswell, E. A., Old, L. J., Kassel, R. L., Green, S., Fiore, N., and Williamson, B. (1975) An endotoxin-induced serum factor that causes necrosis of tumors. *Proc. Natl. Acad. Sci. U. S. A.* **72**, 3666-3670
2. Balkwill, F. (2009) Tumour necrosis factor and cancer. *Nat. Rev. Cancer* **9**, 361-371
3. Aggarwal, B. B., Gupta, S. C., and Kim, J. H. (2012) Historical perspectives on tumor necrosis factor and its superfamily: 25 years later, a golden journey. *Blood* **119**, 651-665
4. Holbrook, J., Lara-Reyna, S., Jarosz-Griffiths, H., and McDermott, M. (2019) Tumour necrosis factor signalling in health and disease. *F1000Res* **8**
5. Kriegler, M., Perez, C., DeFay, K., Albert, I., and Lu, S. D. (1988) A novel form of TNF/cachectin is a cell surface cytotoxic transmembrane protein: ramifications for the complex physiology of TNF. *Cell* **53**, 45-53
6. Jue, D. M., Sherry, B., Luedke, C., Manogue, K. R., and Cerami, A. (1990) Processing of newly synthesized cachectin/tumor necrosis factor in endotoxin-stimulated macrophages. *Biochemistry* **29**, 8371-8377
7. Black, R. A., Rauch, C. T., Kozlosky, C. J., Peschon, J. J., Slack, J. L., Wolfson, M. F., Castner, B. J., Stocking, K. L., Reddy, P., Srinivasan, S., Nelson, N., Boiani, N., Schooley, K. A., Gerhart, M., Davis, R., Fitzner, J. N., Johnson, R. S., Paxton, R. J., March, C. J., and Cerretti, D. P. (1997) A metalloproteinase disintegrin that releases tumour-necrosis factor-alpha from cells. *Nature* **385**, 729-733
8. Sedger, L. M., and McDermott, M. F. (2014) TNF and TNF-receptors: From mediators of cell death and inflammation to therapeutic giants - past, present and future. *Cytokine Growth Factor Rev.* **25**, 453-472
9. Hiscott, J., Marois, J., Garoufalis, J., D'Addario, M., Roulston, A., Kwan, I., Pepin, N., Lacoste, J., Nguyen, H., Bensi, G., and et al. (1993) Characterization of a functional NF-kappa B site in the human interleukin 1 beta promoter: evidence for a positive autoregulatory loop. *Mol. Cell. Biol.* **13**, 6231-6240
10. Paliogianni, F., Raptis, A., Ahuja, S. S., Najjar, S. M., and Boumpas, D. T. (1993) Negative transcriptional regulation of human interleukin 2 (IL-2) gene by glucocorticoids through interference with nuclear transcription factors AP-1 and NF-AT. *J. Clin. Invest.* **91**, 1481-1489
11. Laster, S. M., Wood, J. G., and Gooding, L. R. (1988) Tumor necrosis factor can induce both apoptic and necrotic forms of cell lysis. *J. Immunol.* **141**, 2629-2634
12. Sugarman, B. J., Aggarwal, B. B., Hass, P. E., Figari, I. S., Palladino, M. A., Jr., and Shepard, H. M. (1985) Recombinant human tumor necrosis factor-alpha: effects on proliferation of normal and transformed cells in vitro. *Science* **230**, 943-945
13. Frater-Schroder, M., Risau, W., Hallmann, R., Gautschi, P., and Bohlen, P. (1987) Tumor necrosis factor type alpha, a potent inhibitor of endothelial cell growth in vitro, is angiogenic in vivo. *Proc. Natl. Acad. Sci. U. S. A.* **84**, 5277-5281

14. Verheij, M., Bose, R., Lin, X. H., Yao, B., Jarvis, W. D., Grant, S., Birrer, M. J., Szabo, E., Zon, L. I., Kyriakis, J. M., Haimovitz-Friedman, A., Fuks, Z., and Kolesnick, R. N. (1996) Requirement for ceramide-initiated SAPK/JNK signalling in stress-induced apoptosis. *Nature* **380**, 75-79
15. Sluss, H. K., Barrett, T., Derijard, B., and Davis, R. J. (1994) Signal transduction by tumor necrosis factor mediated by JNK protein kinases. *Mol. Cell. Biol.* **14**, 8376-8384
16. Aoki, H., Kang, P. M., Hampe, J., Yoshimura, K., Noma, T., Matsuzaki, M., and Izumo, S. (2002) Direct activation of mitochondrial apoptosis machinery by c-Jun N-terminal kinase in adult cardiac myocytes. *J. Biol. Chem.* **277**, 10244-10250
17. Scheurich, P., Thoma, B., Ucer, U., and Pfizenmaier, K. (1987) Immunoregulatory activity of recombinant human tumor necrosis factor (TNF)-alpha: induction of TNF receptors on human T cells and TNF-alpha-mediated enhancement of T cell responses. *J. Immunol.* **138**, 1786-1790
18. Vilcek, J., Palombella, V. J., Henriksen-DeStefano, D., Swenson, C., Feinman, R., Hirai, M., and Tsujimoto, M. (1986) Fibroblast growth enhancing activity of tumor necrosis factor and its relationship to other polypeptide growth factors. *J. Exp. Med.* **163**, 632-643
19. Bruggeman, L. A., Drawz, P. E., Kahoud, N., Lin, K., Barisoni, L., and Nelson, P. J. (2011) TNFR2 interposes the proliferative and NF-kappaB-mediated inflammatory response by podocytes to TNF-alpha. *Lab. Invest.* **91**, 413-425
20. Jelinek, D. F., and Lipsky, P. E. (1987) Enhancement of human B cell proliferation and differentiation by tumor necrosis factor-alpha and interleukin 1. *J. Immunol.* **139**, 2970-2976
21. Ligresti, G., Aplin, A. C., Zorzi, P., Morishita, A., and Nicosia, R. F. (2011) Macrophage-derived tumor necrosis factor-alpha is an early component of the molecular cascade leading to angiogenesis in response to aortic injury. *Arterioscler. Thromb. Vasc. Biol.* **31**, 1151-1159
22. Chu, S. C., Tsai, C. H., Yang, S. F., Huang, F. M., Su, Y. F., Hsieh, Y. S., and Chang, Y. C. (2004) Induction of vascular endothelial growth factor gene expression by proinflammatory cytokines in human pulp and gingival fibroblasts. *J. Endod.* **30**, 704-707
23. Maloney, J. P., and Gao, L. (2015) Proinflammatory Cytokines Increase Vascular Endothelial Growth Factor Expression in Alveolar Epithelial Cells. *Mediators Inflamm.* **2015**, 387842
24. Branen, L., Hovgaard, L., Nitulescu, M., Bengtsson, E., Nilsson, J., and Jovinge, S. (2004) Inhibition of tumor necrosis factor-alpha reduces atherosclerosis in apolipoprotein E knockout mice. *Arterioscler. Thromb. Vasc. Biol.* **24**, 2137-2142
25. Canault, M., Peiretti, F., Mueller, C., Kopp, F., Morange, P., Rihs, S., Portugal, H., Juhan-Vague, I., and Nalbone, G. (2004) Exclusive expression of transmembrane TNF-alpha in mice reduces the inflammatory response in early lipid lesions of aortic sinus. *Atherosclerosis* **172**, 211-218
26. Ohta, H., Wada, H., Niwa, T., Kirii, H., Iwamoto, N., Fujii, H., Saito, K., Sekikawa, K., and Seishima, M. (2005) Disruption of tumor necrosis factor-alpha gene diminishes the development of atherosclerosis in ApoE-deficient mice. *Atherosclerosis* **180**, 11-17
27. Barath, P., Fishbein, M. C., Cao, J., Berenson, J., Helfant, R. H., and Forrester, J. S. (1990) Detection and localization of tumor necrosis factor in human atheroma. *Am. J. Cardiol.* **65**, 297-302
28. Barath, P., Fishbein, M. C., Cao, J., Berenson, J., Helfant, R. H., and Forrester, J. S. (1990) Tumor necrosis factor gene expression in human vascular intimal smooth muscle cells detected by in situ hybridization. *Am. J. Pathol.* **137**, 503-509
29. Marui, N., Offermann, M. K., Swerlick, R., Kunsch, C., Rosen, C. A., Ahmad, M., Alexander, R. W., and Medford, R. M. (1993) Vascular cell adhesion molecule-1 (VCAM-1) gene transcription and expression are regulated through an antioxidant-sensitive mechanism in human vascular endothelial cells. *J. Clin. Invest.* **92**, 1866-1874

30. Xia, P., Vadas, M. A., Rye, K. A., Barter, P. J., and Gamble, J. R. (1999) High density lipoproteins (HDL) interrupt the sphingosine kinase signaling pathway. A possible mechanism for protection against atherosclerosis by HDL. *J. Biol. Chem.* **274**, 33143-33147
31. Zeiher, A. M., Fisslthaler, B., Schray-Utz, B., and Busse, R. (1995) Nitric oxide modulates the expression of monocyte chemoattractant protein 1 in cultured human endothelial cells. *Circ. Res.* **76**, 980-986
32. Carr, M. W., Roth, S. J., Luther, E., Rose, S. S., and Springer, T. A. (1994) Monocyte chemoattractant protein 1 acts as a T-lymphocyte chemoattractant. *Proc. Natl. Acad. Sci. U. S. A.* **91**, 3652-3656
33. Deshmane, S. L., Kremlev, S., Amini, S., and Sawaya, B. E. (2009) Monocyte chemoattractant protein-1 (MCP-1): an overview. *J. Interferon Cytokine Res.* **29**, 313-326
34. Schreyer, S. A., Vick, C. M., and LeBoeuf, R. C. (2002) Loss of lymphotoxin-alpha but not tumor necrosis factor-alpha reduces atherosclerosis in mice. *J. Biol. Chem.* **277**, 12364-12368
35. Boesten, L. S., Zadelaar, A. S., van Nieuwkoop, A., Gijbels, M. J., de Winther, M. P., Havekes, L. M., and van Vlijmen, B. J. (2005) Tumor necrosis factor-alpha promotes atherosclerotic lesion progression in APOE*3-Leiden transgenic mice. *Cardiovasc. Res.* **66**, 179-185
36. Schreyer, S. A., Peschon, J. J., and LeBoeuf, R. C. (1996) Accelerated atherosclerosis in mice lacking tumor necrosis factor receptor p55. *J. Biol. Chem.* **271**, 26174-26178
37. Zhang, L., Peppel, K., Sivashanmugam, P., Orman, E. S., Brian, L., Exum, S. T., and Freedman, N. J. (2007) Expression of tumor necrosis factor receptor-1 in arterial wall cells promotes atherosclerosis. *Arterioscler. Thromb. Vasc. Biol.* **27**, 1087-1094
38. Xanthoulea, S., Thelen, M., Pottgens, C., Gijbels, M. J., Lutgens, E., and de Winther, M. P. (2009) Absence of p55 TNF receptor reduces atherosclerosis, but has no major effect on angiotensin II induced aneurysms in LDL receptor deficient mice. *PLoS One* **4**, e6113
39. Blessing, E., Bea, F., Kuo, C. C., Campbell, L. A., Chesebro, B., and Rosenfeld, M. E. (2004) Lesion progression and plaque composition are not altered in older apoE-/- mice lacking tumor necrosis factor-alpha receptor p55. *Atherosclerosis* **176**, 227-232
40. Chandrasekharan, U. M., Mavrakis, L., Bonfield, T. L., Smith, J. D., and DiCorleto, P. E. (2007) Decreased atherosclerosis in mice deficient in tumor necrosis factor-alpha receptor-II (p75). *Arterioscler. Thromb. Vasc. Biol.* **27**, e16-17
41. Quispe, R., Michos, E. D., Martin, S. S., Puri, R., Toth, P. P., Al Suwaidi, J., Banach, M., Virani, S. S., Blumenthal, R. S., Jones, S. R., and Elshazly, M. B. (2020) High-Sensitivity C-Reactive Protein Discordance With Atherogenic Lipid Measures and Incidence of Atherosclerotic Cardiovascular Disease in Primary Prevention: The ARIC Study. *J Am Heart Assoc* **9**, e013600
42. Jovinge, S., Hamsten, A., Tornvall, P., Proudler, A., Bavenholm, P., Ericsson, C. G., Godsland, I., de Faire, U., and Nilsson, J. (1998) Evidence for a role of tumor necrosis factor alpha in disturbances of triglyceride and glucose metabolism predisposing to coronary heart disease. *Metabolism* **47**, 113-118
43. Levine, B., Kalman, J., Mayer, L., Fillit, H. M., and Packer, M. (1990) Elevated circulating levels of tumor necrosis factor in severe chronic heart failure. *N. Engl. J. Med.* **323**, 236-241
44. Paolisso, G., Rizzo, M. R., Mazziotti, G., Tagliamonte, M. R., Gambardella, A., Rotondi, M., Carella, C., Giugliano, D., Varricchio, M., and D'Onofrio, F. (1998) Advancing age and insulin resistance: role of plasma tumor necrosis factor-alpha. *Am. J. Physiol.* **275**, E294-299
45. Rus, H. G., Niculescu, F., and Vlaicu, R. (1991) Tumor necrosis factor-alpha in human arterial wall with atherosclerosis. *Atherosclerosis* **89**, 247-254
46. Gordon, T., Castelli, W. P., Hjortland, M. C., Kannel, W. B., and Dawber, T. R. (1977) High density lipoprotein as a protective factor against coronary heart disease. The Framingham Study. *Am. J. Med.* **62**, 707-714

47. Zhang, Y., Vittinghoff, E., Pletcher, M. J., Allen, N. B., Zeki Al Hazzouri, A., Yaffe, K., Balte, P. P., Alonso, A., Newman, A. B., Ives, D. G., Rana, J. S., Lloyd-Jones, D., Vasan, R. S., Bibbins-Domingo, K., Gooding, H. C., de Ferranti, S. D., Oelsner, E. C., and Moran, A. E. (2019) Associations of Blood Pressure and Cholesterol Levels During Young Adulthood With Later Cardiovascular Events. *J. Am. Coll. Cardiol.* **74**, 330-341
48. Niemann-Jonsson, A., Dimayuga, P., Jovinge, S., Calara, F., Ares, M. P., Fredrikson, G. N., and Nilsson, J. (2000) Accumulation of LDL in rat arteries is associated with activation of tumor necrosis factor-alpha expression. *Arterioscler. Thromb. Vasc. Biol.* **20**, 2205-2211
49. Byl, B., Roucloux, I., Crusiaux, A., Dupont, E., and Deviere, J. (1993) Tumor necrosis factor alpha and interleukin 6 plasma levels in infected cirrhotic patients. *Gastroenterology* **104**, 1492-1497
50. Gimbrone, M. A., Jr., and Garcia-Cardena, G. (2016) Endothelial Cell Dysfunction and the Pathobiology of Atherosclerosis. *Circ. Res.* **118**, 620-636
51. Ross, R., Wight, T. N., Strandness, E., and Thiele, B. (1984) Human atherosclerosis. I. Cell constitution and characteristics of advanced lesions of the superficial femoral artery. *Am. J. Pathol.* **114**, 79-93
52. Hoff, H. F., and Morton, R. E. (1985) Lipoproteins containing apo B extracted from human aortas. Structure and function. *Ann. N. Y. Acad. Sci.* **454**, 183-194
53. Mahley, R. W., Innerarity, T. L., Weisgraber, K. H., and Fry, D. L. (1977) Canine hyperlipoproteinemia and atherosclerosis. Accumulation of lipid by aortic medial cells in vivo and in vitro. *Am. J. Pathol.* **87**, 205-226
54. Vlodavsky, I., Fielding, P. E., Fielding, C. J., and Gospodarowicz, D. (1978) Role of contact inhibition in the regulation of receptor-mediated uptake of low density lipoprotein in cultured vascular endothelial cells. *Proc. Natl. Acad. Sci. U. S. A.* **75**, 356-360
55. Poole, J. C., and Florey, H. W. (1958) Changes in the endothelium of the aorta and the behaviour of macrophages in experimental atheroma of rabbits. *J. Pathol. Bacteriol.* **75**, 245-251
56. Simionescu, M. (2007) Implications of early structural-functional changes in the endothelium for vascular disease. *Arterioscler. Thromb. Vasc. Biol.* **27**, 266-274
57. Joris, I., Zand, T., Nunnari, J. J., Krolikowski, F. J., and Majno, G. (1983) Studies on the pathogenesis of atherosclerosis. I. Adhesion and emigration of mononuclear cells in the aorta of hypercholesterolemic rats. *Am. J. Pathol.* **113**, 341-358
58. Satriano, J. A., Shuldiner, M., Hora, K., Xing, Y., Shan, Z., and Schlondorff, D. (1993) Oxygen radicals as second messengers for expression of the monocyte chemoattractant protein, JE/MCP-1, and the monocyte colony-stimulating factor, CSF-1, in response to tumor necrosis factor-alpha and immunoglobulin G. Evidence for involvement of reduced nicotinamide adenine dinucleotide phosphate (NADPH)-dependent oxidase. *J. Clin. Invest.* **92**, 1564-1571
59. Ding, A. H., Nathan, C. F., and Stuehr, D. J. (1988) Release of reactive nitrogen intermediates and reactive oxygen intermediates from mouse peritoneal macrophages. Comparison of activating cytokines and evidence for independent production. *J. Immunol.* **141**, 2407-2412
60. Trinh, M. N., Brown, M. S., Goldstein, J. L., Han, J., Vale, G., McDonald, J. G., Seemann, J., Mendell, J. T., and Lu, F. (2020) Last step in the path of LDL cholesterol from lysosome to plasma membrane to ER is governed by phosphatidylserine. *Proc. Natl. Acad. Sci. U. S. A.* **117**, 18521-18529
61. Acton, S. L., Scherer, P. E., Lodish, H. F., and Krieger, M. (1994) Expression cloning of SR-BI, a CD36-related class B scavenger receptor. *J. Biol. Chem.* **269**, 21003-21009
62. Brundert, M., Ewert, A., Heeren, J., Behrendt, B., Ramakrishnan, R., Greten, H., Merkel, M., and Rinninger, F. (2005) Scavenger receptor class B type I mediates the selective uptake of high-density lipoprotein-associated cholesteryl ester by the liver in mice. *Arterioscler. Thromb. Vasc. Biol.* **25**, 143-148

63. Connelly, M. A., Kellner-Weibel, G., Rothblat, G. H., and Williams, D. L. (2003) SR-BI-directed HDL-cholesteryl ester hydrolysis. *J. Lipid Res.* **44**, 331-341
64. Shan, L., Pang, L., Zhang, R., Murgolo, N. J., Lan, H., and Hedrick, J. A. (2008) PCSK9 binds to multiple receptors and can be functionally inhibited by an EGF-A peptide. *Biochem. Biophys. Res. Commun.* **375**, 69-73
65. Poirier, S., Mayer, G., Benjannet, S., Bergeron, E., Marcinkiewicz, J., Nassoury, N., Mayer, H., Nimpf, J., Prat, A., and Seidah, N. G. (2008) The proprotein convertase PCSK9 induces the degradation of low density lipoprotein receptor (LDLR) and its closest family members VLDLR and ApoER2. *J. Biol. Chem.* **283**, 2363-2372
66. Canuel, M., Sun, X., Asselin, M. C., Paramithiotis, E., Prat, A., and Seidah, N. G. (2013) Proprotein convertase subtilisin/kexin type 9 (PCSK9) can mediate degradation of the low density lipoprotein receptor-related protein 1 (LRP-1). *PLoS One* **8**, e64145
67. Ruiz, J., Kouiavskaia, D., Migliorini, M., Robinson, S., Saenko, E. L., Gorlatova, N., Li, D., Lawrence, D., Hyman, B. T., Weisgraber, K. H., and Strickland, D. K. (2005) The apoE isoform binding properties of the VLDL receptor reveal marked differences from LRP and the LDL receptor. *J. Lipid Res.* **46**, 1721-1731
68. Herz, J., Goldstein, J. L., Strickland, D. K., Ho, Y. K., and Brown, M. S. (1991) 39-kDa protein modulates binding of ligands to low density lipoprotein receptor-related protein/alpha 2-macroglobulin receptor. *J. Biol. Chem.* **266**, 21232-21238
69. Holtzman, D. M., Herz, J., and Bu, G. (2012) Apolipoprotein E and apolipoprotein E receptors: normal biology and roles in Alzheimer disease. *Cold Spring Harb. Perspect. Med.* **2**, a006312
70. Lei, L., Xiong, Y., Chen, J., Yang, J. B., Wang, Y., Yang, X. Y., Chang, C. C., Song, B. L., Chang, T. Y., and Li, B. L. (2009) TNF-alpha stimulates the ACAT1 expression in differentiating monocytes to promote the CE-laden cell formation. *J. Lipid Res.* **50**, 1057-1067
71. An, S., Jang, Y. S., Park, J. S., Kwon, B. M., Paik, Y. K., and Jeong, T. S. (2008) Inhibition of acyl-coenzyme A:cholesterol acyltransferase stimulates cholesterol efflux from macrophages and stimulates farnesoid X receptor in hepatocytes. *Exp. Mol. Med.* **40**, 407-417
72. Henriksen, T., Mahoney, E. M., and Steinberg, D. (1981) Enhanced macrophage degradation of low density lipoprotein previously incubated with cultured endothelial cells: recognition by receptors for acetylated low density lipoproteins. *Proc. Natl. Acad. Sci. U. S. A.* **78**, 6499-6503
73. Goldstein, J. L., Hoff, H. F., Ho, Y. K., Basu, S. K., and Brown, M. S. (1981) Stimulation of cholesteryl ester synthesis in macrophages by extracts of atherosclerotic human aortas and complexes of albumin/cholesteryl esters. *Arteriosclerosis* **1**, 210-226
74. Khoo, J. C., Miller, E., McLoughlin, P., and Steinberg, D. (1988) Enhanced macrophage uptake of low density lipoprotein after self-aggregation. *Arteriosclerosis* **8**, 348-358
75. Hurt, E., and Camejo, G. (1987) Effect of arterial proteoglycans on the interaction of LDL with human monocyte-derived macrophages. *Atherosclerosis* **67**, 115-126
76. Salisbury, B. G., Falcone, D. J., and Minick, C. R. (1985) Insoluble low-density lipoprotein-proteoglycan complexes enhance cholesteryl ester accumulation in macrophages. *Am. J. Pathol.* **120**, 6-11
77. Hurt, E., Bondjers, G., and Camejo, G. (1990) Interaction of LDL with human arterial proteoglycans stimulates its uptake by human monocyte-derived macrophages. *J. Lipid Res.* **31**, 443-454
78. Paone, S., Baxter, A. A., Hulett, M. D., and Poon, I. K. H. (2019) Endothelial cell apoptosis and the role of endothelial cell-derived extracellular vesicles in the progression of atherosclerosis. *Cell. Mol. Life Sci.* **76**, 1093-1106

79. Dehouck, B., Fenart, L., Dehouck, M. P., Pierce, A., Torpier, G., and Cecchelli, R. (1997) A new function for the LDL receptor: transcytosis of LDL across the blood-brain barrier. *J. Cell Biol.* **138**, 877-889
80. Vasile, E., Simionescu, M., and Simionescu, N. (1983) Visualization of the binding, endocytosis, and transcytosis of low-density lipoprotein in the arterial endothelium in situ. *J. Cell Biol.* **96**, 1677-1689
81. Acton, S., Rigotti, A., Landschulz, K. T., Xu, S., Hobbs, H. H., and Krieger, M. (1996) Identification of scavenger receptor SR-BI as a high density lipoprotein receptor. *Science* **271**, 518-520
82. Swarnakar, S., Temel, R. E., Connelly, M. A., Azhar, S., and Williams, D. L. (1999) Scavenger receptor class B, type I, mediates selective uptake of low density lipoprotein cholesteryl ester. *J. Biol. Chem.* **274**, 29733-29739
83. Rohrer, L., Ohnsorg, P. M., Lehner, M., Landolt, F., Rinninger, F., and von Eckardstein, A. (2009) High-density lipoprotein transport through aortic endothelial cells involves scavenger receptor BI and ATP-binding cassette transporter G1. *Circ. Res.* **104**, 1142-1150
84. Fisher, C., Beglova, N., and Blacklow, S. C. (2006) Structure of an LDLR-RAP complex reveals a general mode for ligand recognition by lipoprotein receptors. *Mol. Cell* **22**, 277-283
85. Flynn, J. L., Goldstein, M. M., Chan, J., Triebold, K. J., Pfeffer, K., Lowenstein, C. J., Schreiber, R., Mak, T. W., and Bloom, B. R. (1995) Tumor necrosis factor-alpha is required in the protective immune response against Mycobacterium tuberculosis in mice. *Immunity* **2**, 561-572
86. Josephs, S. F., Ichim, T. E., Prince, S. M., Kesari, S., Marincola, F. M., Escobedo, A. R., and Jafri, A. (2018) Unleashing endogenous TNF-alpha as a cancer immunotherapeutic. *J. Transl. Med.* **16**, 242
87. Seo, S. H., and Webster, R. G. (2002) Tumor necrosis factor alpha exerts powerful anti-influenza virus effects in lung epithelial cells. *J. Virol.* **76**, 1071-1076
88. Del Valle, D. M., Kim-Schulze, S., Hsin-Hui, H., Beckmann, N. D., Nirenberg, S., Wang, B., Lavin, Y., Swartz, T., Madduri, D., Stock, A., Marron, T., Xie, H., Patel, M. K., van Oekelen, O., Rahman, A., Kovatch, P., Aberg, J., Schadt, E., Jagannath, S., Mazumdar, M., Charney, A., Firpo-Betancourt, A., Mendu, D. R., Jhang, J., Reich, D., Sigel, K., Cordon-Cardo, C., Feldmann, M., Parekh, S., Merad, M., and Gnjatic, S. (2020) An inflammatory cytokine signature helps predict COVID-19 severity and death. *medRxiv*
89. Gerriets, V., Bansal, P., Goyal, A., and Khaddour, K. (2020) Tumor Necrosis Factor Inhibitors. in *StatPearls*, Treasure Island (FL). pp
90. Mahley, R. W., and Weisgraber, K. H. (1974) Canine lipoproteins and atherosclerosis. I. Isolation and characterization of plasma lipoproteins from control dogs. *Circ. Res.* **35**, 713-721
91. Kovanen, P. T., Brown, M. S., Basu, S. K., Bilheimer, D. W., and Goldstein, J. L. (1981) Saturation and suppression of hepatic lipoprotein receptors: a mechanism for the hypercholesterolemia of cholesterol-fed rabbits. *Proc. Natl. Acad. Sci. U. S. A.* **78**, 1396-1400
92. Sparrow, C. P., and Pittman, R. C. (1990) Cholesterol esters selectively taken up from high-density lipoproteins are hydrolyzed extralysosomally. *Biochim. Biophys. Acta* **1043**, 203-210
93. Gerbod-Giannone, M. C., Li, Y., Holleboom, A., Han, S., Hsu, L. C., Tabas, I., and Tall, A. R. (2006) TNFalpha induces ABCA1 through NF-kappaB in macrophages and in phagocytes ingesting apoptotic cells. *Proc. Natl. Acad. Sci. U. S. A.* **103**, 3112-3117
94. Kume, N., Murase, T., Moriwaki, H., Aoyama, T., Sawamura, T., Masaki, T., and Kita, T. (1998) Inducible expression of lectin-like oxidized LDL receptor-1 in vascular endothelial cells. *Circ. Res.* **83**, 322-327
95. Nagase, M., Ando, K., Nagase, T., Kaname, S., Sawamura, T., and Fujita, T. (2001) Redox-sensitive regulation of lox-1 gene expression in vascular endothelium. *Biochem. Biophys. Res. Commun.* **281**, 720-725

96. Sakashita, N., Chang, C. C., Lei, X., Fujiwara, Y., Takeya, M., and Chang, T. Y. (2010) Cholesterol loading in macrophages stimulates formation of ER-derived vesicles with elevated ACAT1 activity. *J. Lipid Res.* **51**, 1263-1272
97. Havel, R., Eder, H., and Bragdon, J. (1955) The distribution and chemical composition of ultracentrifugally separated lipoproteins in human serum. *J Clin. Invest.* **34**, 1345-1353
98. Skipski, V. P., Barclay, M., Barclay, R. K., Fetzer, V. A., Good, J. J., and Archibald, F. M. (1967) Lipid composition of human serum lipoproteins. *Biochem. J.* **104**, 340-352
99. Kuchinskiene, Z., and Carlson, L. A. (1982) Composition, concentration, and size of low density lipoproteins and of subfractions of very low density lipoproteins from serum of normal men and women. *J. Lipid Res.* **23**, 762-769
100. Mahley, R. W., Innerarity, T. L., Rall, S. C., Jr., and Weisgraber, K. H. (1984) Plasma lipoproteins: apolipoprotein structure and function. *J. Lipid Res.* **25**, 1277-1294
101. Andreae, W. A. (1955) A sensitive method for the estimation of hydrogen peroxide in biological materials. *Nature* **175**, 859-860
102. Allain, C. C., Poon, L. S., Chan, C. S., Richmond, W., and Fu, P. C. (1974) Enzymatic determination of total serum cholesterol. *Clin. Chem.* **20**, 470-475
103. Bligh, E. G., and Dyer, W. J. (1959) A rapid method of total lipid extraction and purification. *Can. J. Biochem. Physiol.* **37**, 911-917
104. Kaluzny, M. A., Duncan, L. A., Merritt, M. V., and Epps, D. E. (1985) Rapid separation of lipid classes in high yield and purity using bonded phase columns. *J. Lipid Res.* **26**, 135-140
105. Pitas, R. E., Innerarity, T. L., Weinstein, J. N., and Mahley, R. W. (1981) Acetoacetylated lipoproteins used to distinguish fibroblasts from macrophages in vitro by fluorescence microscopy. *Arteriosclerosis* **1**, 177-185
106. Burstein, M., Scholnick, H. R., and Morfin, R. (1970) Rapid method for the isolation of lipoproteins from human serum by precipitation with polyanions. *J. Lipid Res.* **11**, 583-595
107. McQuin, C., Goodman, A., Chernyshev, V., Kamentsky, L., Cimini, B. A., Karhohs, K. W., Doan, M., Ding, L., Rafelski, S. M., Thirstrup, D., Wiegraebe, W., Singh, S., Becker, T., Caicedo, J. C., and Carpenter, A. E. (2018) CellProfiler 3.0: Next-generation image processing for biology. *PLoS Biol.* **16**, e2005970

FOOTNOTES

Abbreviations: ACAT, acyl-CoA cholesterol acyltransferase; AP, apical; apoE , apolipoprotein E; BHT, butylated hydroxytoluene; BL, basolateral; CAB, cholesterol assay buffer, DB, dialysis buffer; DiL, 1,1′-Dioctadecyl-3,3,3′,3′-tetramethylindocarbocyanine perchlorate; DMSO, dimethyl sulfoxide; GAPDH, glyceraldehyde 3-phosphate dehydrogenase; FAF-BSA, fatty acid-free bovine serum albumin; FBS, fetal bovine serum; LDLR, low density lipoprotein receptor; LRP, ldlr- related protein; mHBSS, modified Hanks' balanced salt solution; PBS, phosphate buffered saline; PCSK9, proprotein convertase subtilisin/kexin type 9; PhenA, 1,10-phenanthroline; pHAECs, primary human aortic endothelial cells; RAP, receptor associated protein; SDS, sodium dodecyl sulfate; TMTU, tetramethylthiourea; TNFα, tumor necrosis factor alpha; VBM, vascular basal medium; VEGF, vascular endothelial growth factor kit;

FIGURE LEGENDS

Figure 1. TNFα enhances cholesterol accumulation and LDL binding to pHAECs. A-B, The pHAECs in serum-free, growth factor-containing medium were treated with the indicted concentration of human LDL without (Ctrl) or with 100 ng/ml TNFα for 24 hours. Unesterified cholesterol and cholesteryl

esters were determined as described under Experimental Procedures. The data represent 5 independent experiments. **C**, Confluent pHAECs were pre-treated with 0 or 5 ng/ml TNFα in serum medium as described under Experimental Procedures. The amount of ^{125}I-LDL released to serum-free medium at 4 ºC without (0) or with 20 folds unlabeled LDL competitor (+) was determined as the surface ^{125}I-LDL. **D**, The experiment was performed as in E, and the amount of radioactivity associated with the cell was determined. C-D are representative of 3 experiments. Error bars represent standard deviations. *,**,***, p< 0.05, 0.01, 0.001, respectively, relative to the corresponding Ctrl.

Figure 2. LDL oxidation is not required for TNFα-induced LDL binding and internalization. A-B, Cells were treated with 0 (Ctrl) or 100 ng/ml TNFα (TNFα) for 24 hrs in serum medium. The media were replaced with serum-free media in the continued presence of TNFα for 2 hrs to remove surface lipoproteins. Finally, 2 µg/ml dil-LDL in serum-free medium (Dil-LDL) containing 40 times LDL (+40X LDL) or oxLDL (+40X oxLDL) was added. Following 2 hr incubation, the cells were washed 3X with mHBSS, then fixed with paraformaldehyde. Images in A are typical of 3 independent experiments, B. Error bars represent standard deviations. **C**, Coomassie stain of two batches of electrophoresed LDL and oxLDL proteins isolated during the course of the experiments. Positions of apoB and apoE are indicated.

Figure 3. TNFα induces massive Dil over [^{3}H]CE lipid accumulation from LDL. pHAECs in serum medium were pre-treated with the indicated concentration of human TNFα for 24 hrs. Subsequently, the cells were treated in the continued presence of the previous TNFα concentration and 50 µg/ml [^{3}H]CE-LDL (**A**) or 5 µg/ml Dil-LDL (**B**) without serum. 24 hrs later, the cells were washed with heparin as described under Experimental Procedures. **C**, The cells were treated without (Ctrl) or with 100 ng/ml TNFα, as above (**D**) in the presence of increasing concentration of Dil-LDL. The data are representative of 3-5 independent experiments performed in triplicates or greater. Error bars represent standard deviations. *,**,*** ,p< 0.05, 0.01, 0.001, respectively, relative to 0 ng/ml TNFα or Dil-LDL. ##, p< 0.01, relative to the previous TNFα dose. $$$, p< 0.001, relative to the corresponding Dil-LDL concentration under Ctrl condition.

Figure 4. Blockage of endosomal acidification enhances TNFα-induced LDL lipid accumulation. The cells were pre-treated with 0 or 100 ng/ml TNFα (+) for 24 hrs in the presence of serum. Subsequently, in the continued presence of TNFα, the cells were treated with 0.5 µg/ml Dil-LDL, plus 50 or 200 µg/ml [^{3}H]CE-LDL, and containing 0 or 50 µM chloroquine diphosphate (Cl-quine), +, an endosomal deacidifier, without serum. After 24 hrs, the intracellular fluorescence (**A-B**) or radioactivity (**C**) was determined. The separation of cells in A is an artificact of preparation prior to lysing the cells for radioactivity. The circumferential accumulation of the Dil-LDL upon raising the endosomal pH is apparent in A. The images are 20X magnifications. Error bars represent standard deviations. The data are representative of 2 independent experiments performed in triplicates without significant variation.

Figure 5. Effect of native lipoprotein receptors on Dil-LDL cell association in pHAECs and hepatocytes. A-B, pHAECs in serum medium were pre-treated with 0 or 100 ng/ml TNFα for 24 hrs. Afterwards, the cells were cultured in the presence of 0.05% DMSO vehicle, or the vehicle plus 50 µM BLT-1 (SR-B1 inhibitor), 12.5 µg/ml human PCSK9 (ApoER, LDLR, LRP, and VLDLR inhibitor), or 21 µg/ml human RAP (ApoER2, LRP, and VLDLR inhibitor) in serum-free medium for 1 hr. Lastly, 8 µg/ml dil-LDL was added, followed by 4 hr incubation. The data are representative of 3 independent experiments. **C**, Mouse immorto hepatocytes were incubated in serum-free RPMI 1640 medium containing the indicated inhibitors as above for 1 hr. Lastly, the hepatocytes were incubated with 10

µg/ml dil-HDL3, -LDL, or apoE-VLDL, as indicated, for 2 hrs. Error bars represent standard deviations.**,***, p< 0.01, 0.001, respectively. NS = not significant.

Figure 6. TNFα increases surface-accessible LDLR without a significant change in total protein. A-B, Confluent pHAECs were pre-treated with 0 or 100 ng/ml TNFa (+) in serum medium for 24 hrs. The cells were then cultured in serum-free medium in the continued presence of TNFα without any antibody (None), 18 µg/ml normal goat IgG control (Ctrl) or goat LDLR antibody (LDLR) for 3 hrs. Cellular LDLR and GAPDH were detected by immunoblottig. It can be seen in A that the LDLR Ab is selective for the LDLR. The data are representative of 3 independent experiments. Error bars represent standard deviations. NS = not significant.

Figure 7. TNFα-induced dil-LDL and apoE-VLDL cell association are blocked by specific LDLR Antibody. Confluent pHAECs in serum medium were pre-treated with 0 (Ctrl) or 100 ng/ml TNFα (TNFα) for 24 hrs. Subsequently, in the continued presence of TNFα, the media were replaced with 20 µg/ml control normal goat IgG (NG IgG) or LDLR antibody (LDLR Ab) for 1 hr without serum. Afterwards, Dil-HDL3 (**A-B**), Dil-LDL (**C-D**), or Dil-apoE3-VLDL (**E-F**) were added to 10 µg/ml. Following 2 hr incubation, cell-associated Dil-lipoproteins were determined. The images are from a single experiment, representative of 4 independent experiments. The images are 20X magnifications. Error bars represent standard deviations.***, p< 0.001 relative to NG IgG.

Figure 8. TNFα induces surface redistribution of LDLR. Confluent pHAECs in serum medium were pre-treated with 0 (Ctrl) or 100 ng/ml TNFα (TNFα) for 24 hrs. Subsequently, in the continued presence of TNFα, the media were replaced with 5 µg/ml control normal goat IgG or LDLR antibody (LDLR Ab) for 0, 5, 30, or 120 minutes at 37 °C. The surface-accessible LDLR was then determined as detailed under Experimental Procedures. **A**, 20X objective magnification of LDLR detected after 30 minutes. **B**, 40X confocal detection of LDLR in TNFα-treated pHAECs at 0 and 5 minutes. The arrows show the membrane distribution of the LDLR in focus, while the arrowhead shows internalized LDLR. **C**, Surface-accessible LDLR as a function of time under control condition. **D**, As C, in the presence of TNFα. The data are representative of 4 independent experiments. Error bars represent standard deviations. **, p< 0.01 relative to control at the same time.

Figure 9. ACAT inhibitor does not prevent TNFα-induced LDL cholesterol accumulation. Confluent pHAECs in serum-free medium were treated with 0 or 100 ng/ml TNFα in the presence of 0.1% DMSO (DMSO) or 10 µg/ml ACAT inhibitor (Sandoz 58-035) and 100 µg/ml LDL for 24 hrs. After washing with heparin as described under Experimental Procedures, the cellular cholesterol content was determined. The data are representative of 3 independent experiments. Error bars represent standard deviations.*,**,***, p< 0.05, 0.01, 0.001, respectively, relative to corresponding Ctrl or as indicated with bars.

Figure 10. TNFα does not affect AP to BL release of degraded LDL protein. A, Diagram of the experimental setup in B-C, in which pHAECs were grown to confluence on 3 µm polycarbonate filters, with ^{125}I-LDL in the AP medium. **B**, pHAECs in serum medium were pre-treated with 0 (Ctrl) or 5 ng/ml TNFα on the BL side for 48 hrs. Then 10 µg/ml ^{125}I-LDL without serum was added to the AP side (No Competitor) or with 30 folds unlabeled LDL (Unlabeled Competitor), in the continued presence of TNFα. After 3 hours, the BL media were collected, and non-intact ^{125}I-LDL was measured as described under Experimental Procedures. **C**, The experiment was performed as in B, followed by detection of

intact BL ^{125}I-LDL. The data are representative of 3 independent experiments. Error bars represent standard deviations.*,**, p< 0.05, 0.01, respectively,

Figure 11. TNFα does not affect AP to BL LDL lipid release. A-D, pHAECs were pre-treated as in Figure 10 with 0, 10, or 100 ng/ml TNFα for 24 hrs in serum. Subsequently, 20 µg/ml control normal goat IgG (Goat IgG) or LDLR antibody (LDLR Ab) was added to the AP medium without serum for 2 hrs. Finally, 1.6 mg/ml double labeled Dil,[^{3}H]CE-LDL was added to the AP medium for 3 hrs. After heparin wash, the intracellular fluorescence (**A-B**), ^{3}H radioactivity (**C**), or medium BL ^{3}H (**D**) was determined. **E**, The cells were treated for 3 or 24 hrs with 0 (Ctrl) or 100 ng/ml TNFα without serum in the presence of apical Dil-LDL, and the BL fluorescence was determined. The images in A are from a single experiment. The data are representative of 3 independent experiments. Error bars represent standard deviations. NS = not significant.

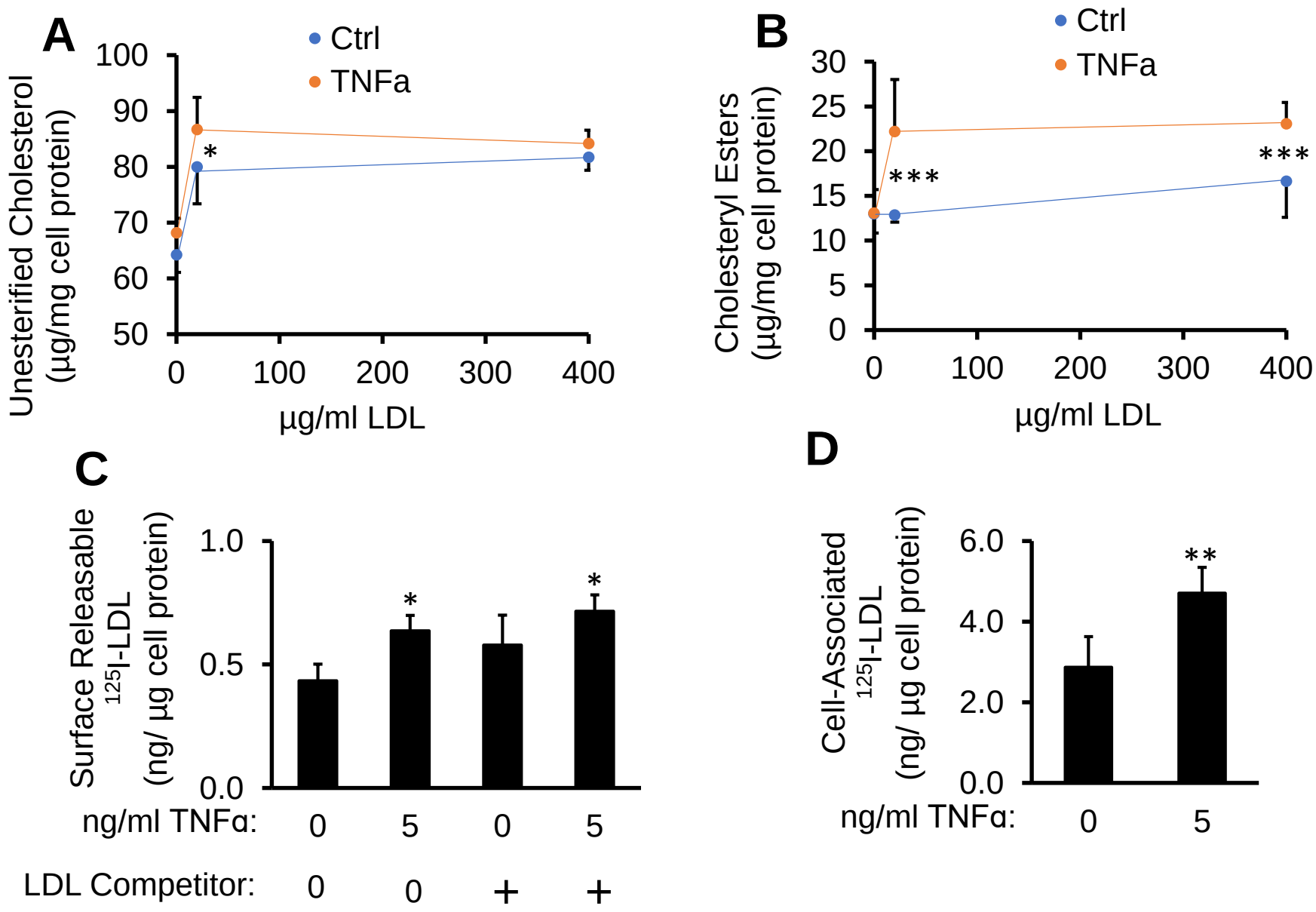
A
Ctrl
TNFa
Unesterified Cholesterol (µg/mg cell protein)
100
90
80
70
60
50
0
100
200
300
400
µg/ml LDL
*
B
Ctrl
TNFa
Cholesteryl Esters (µg/mg cell protein)
30
25
20
15
10
5
0
0
100
200
300
400
µg/ml LDL
***
***
C
Surface Releasable 125I-LDL (ng/ µg cell protein)
1.0
0.5
0.0
*
*
ng/ml TNFα: 0 5 0 5
LDL Competitor: 0 0 + +
D
Cell-Associated 125I-LDL (ng/ µg cell protein)
6.0
4.0
2.0
0.0
**
ng/ml TNFα: 0 5

Figure 1

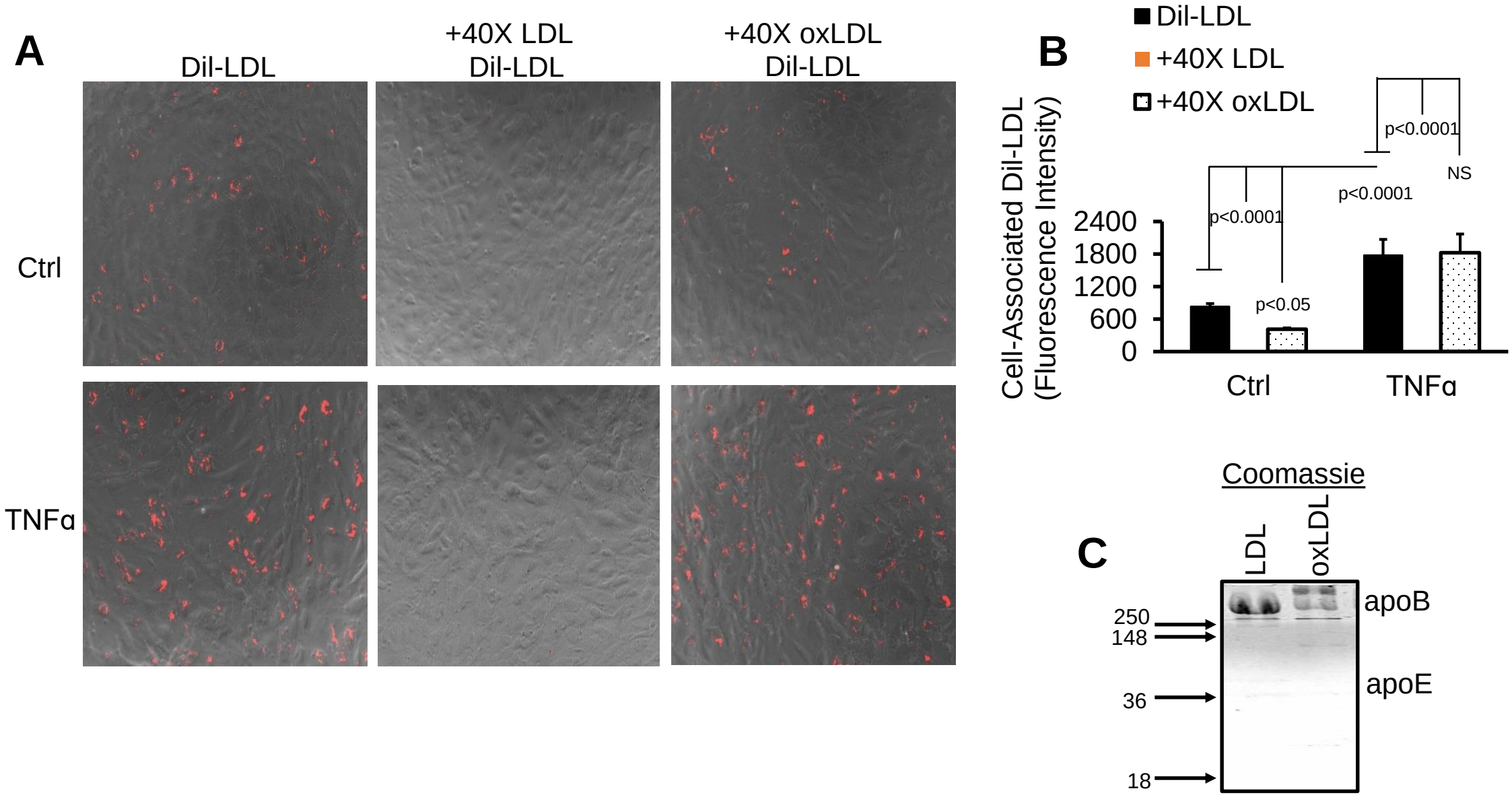
A
Dil-LDL
+40X LDL
Dil-LDL
+40X oxLDL
Dil-LDL
Ctrl
TNFα
B
Dil-LDL
+40X LDL
+40X oxLDL
Cell-Associated Dil-LDL
(Fluorescence Intensity)
2400
1800
1200
600
0
p<0.0001
NS
p<0.0001
p<0.0001
p<0.05
Ctrl
TNFα
C
Coomassie
LDL
oxLDL
250
148
36
18
apoB
apoE

Figure 2

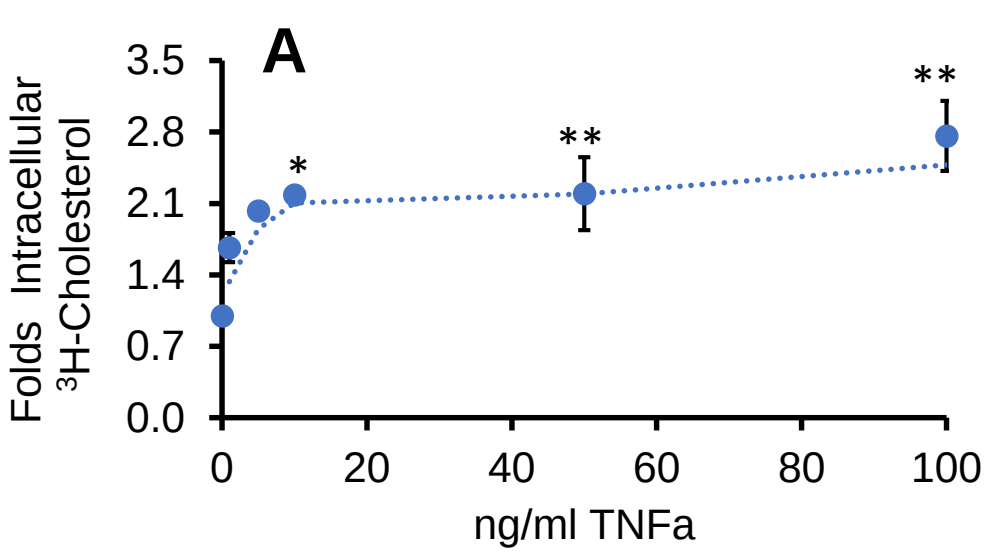
A
Folds Intracellular
^{3}H-Cholesterol
3.5
2.8
2.1
1.4
0.7
0.0
0
20
40
60
80
100
ng/ml TNFa
*
**
**

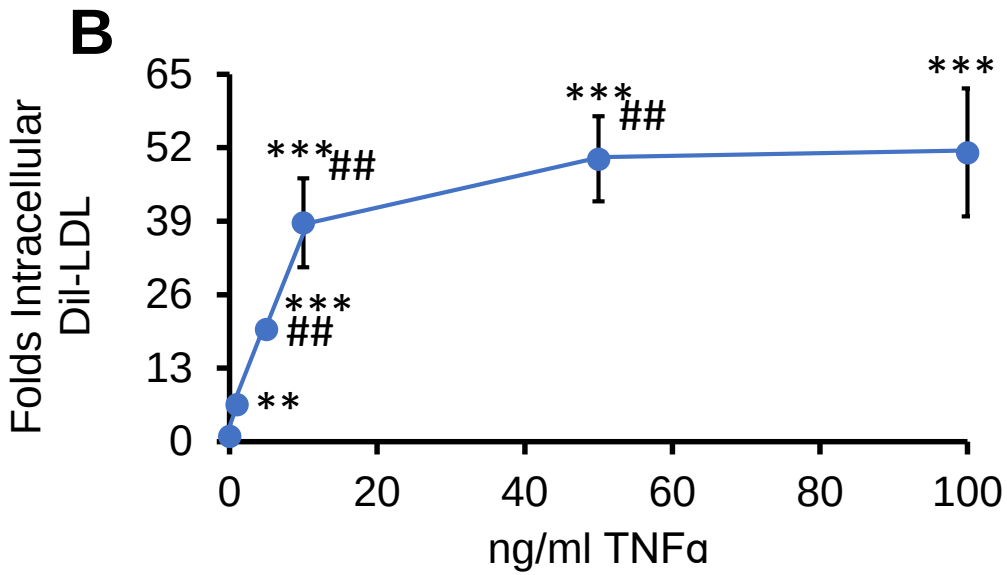
B
Folds Intracellular
DiI-LDL
65
52
39
26
13
0
0
20
40
60
80
100
ng/ml TNFα
**
***
##
***
##
***
##

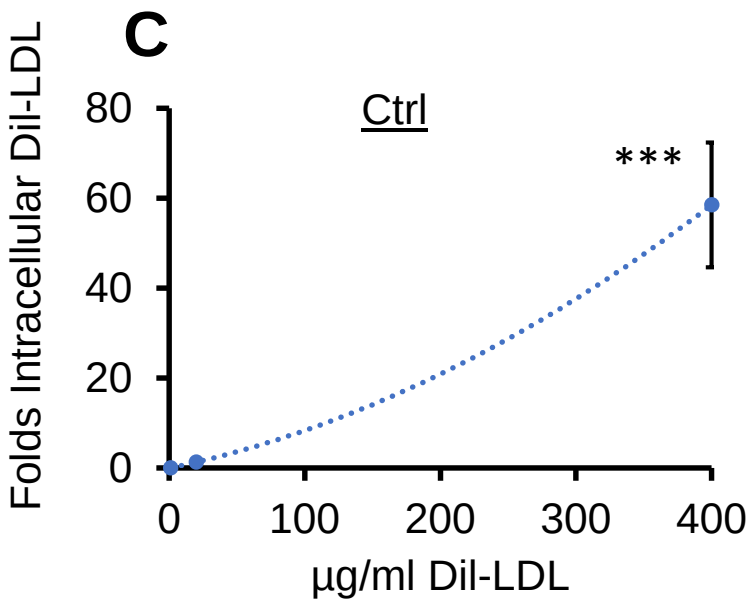
C
Folds Intracellular DiI-LDL
80
60
40
20
0
0
100
200
300
400
µg/ml DiI-LDL
Ctrl
***

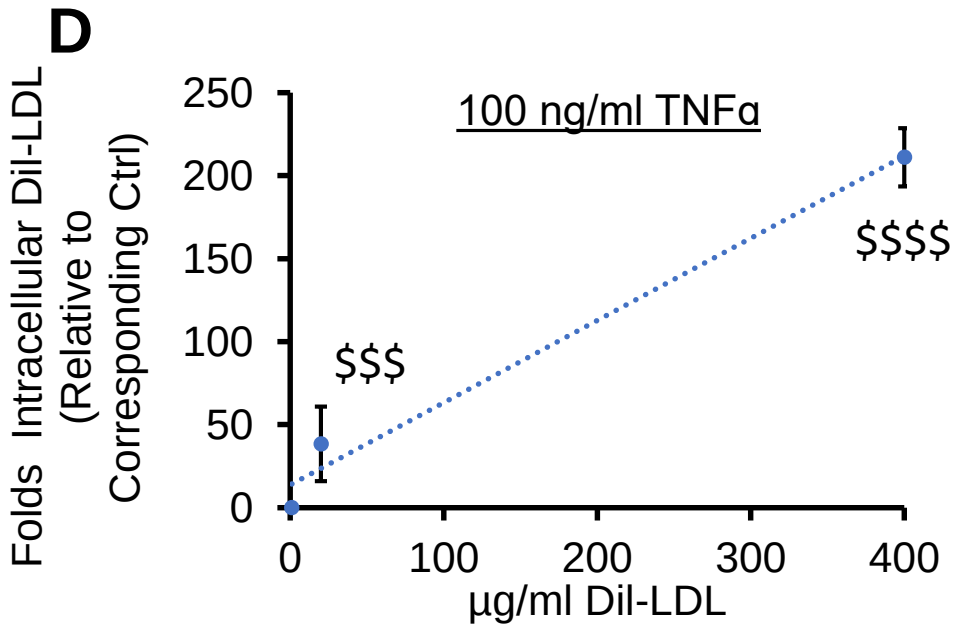
D
Folds Intracellular DiI-LDL
(Relative to
Corresponding Ctrl)
250
200
150
100
50
0
0
100
200
300
400
µg/ml DiI-LDL
100 ng/ml TNFα
$$$
$$$$

Figure 3

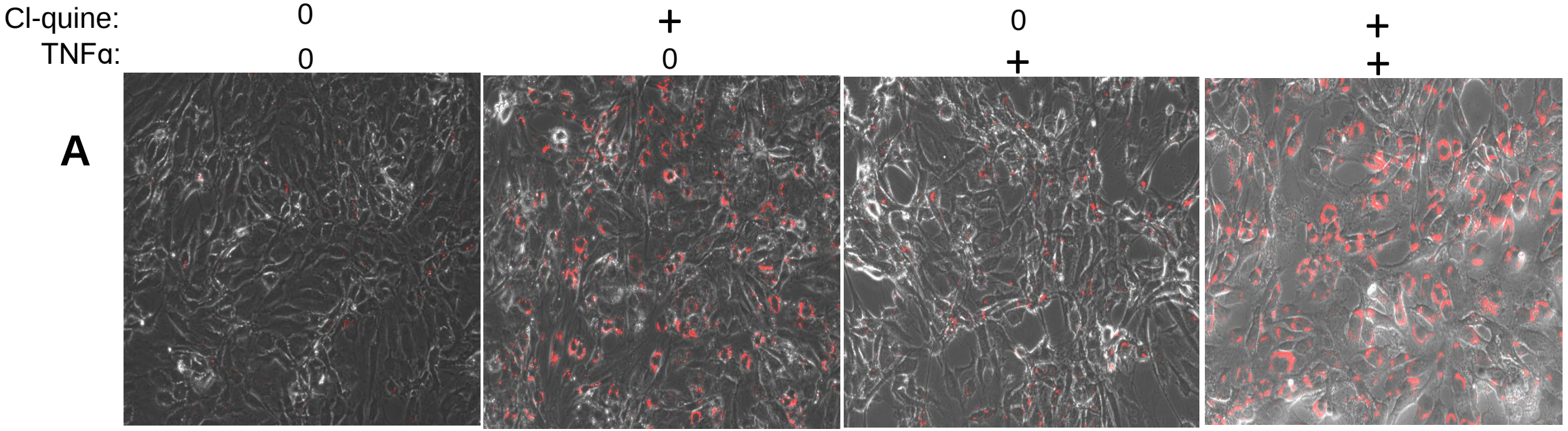
Cl-quine: 0 + 0 +
TNFα: 0 0 + +
A

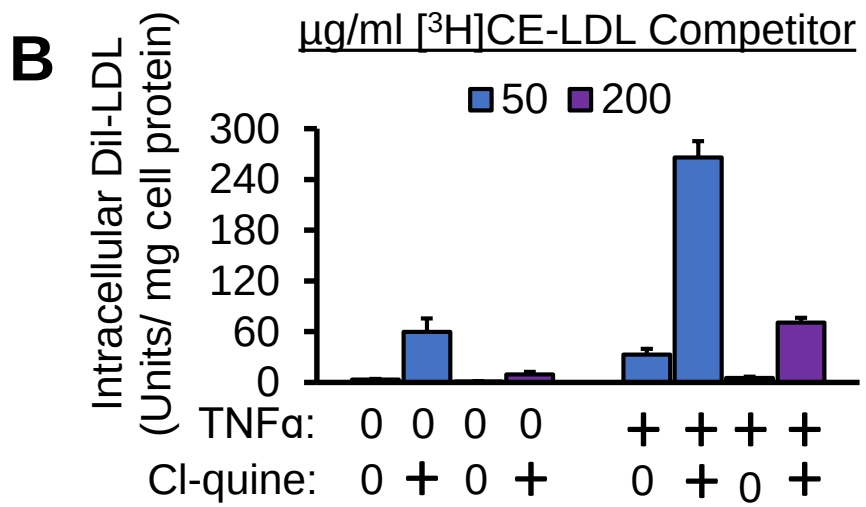
B
µg/ml [3H]CE-LDL Competitor
50 200
Intracellular DiI-LDL (Units/ mg cell protein)
300
240
180
120
60
0
TNFα: 0 0 0 0 + + + +
Cl-quine: 0 + 0 + 0 + 0 +

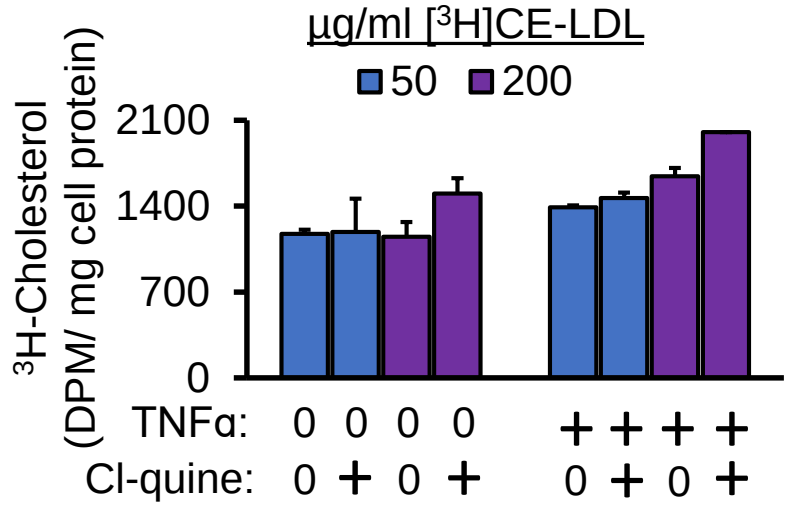
C
µg/ml [3H]CE-LDL
50 200
3H-Cholesterol (DPM/ mg cell protein)
2100
1400
700
0
TNFα: 0 0 0 0 + + + +
Cl-quine: 0 + 0 + 0 + 0 +

Figure 4

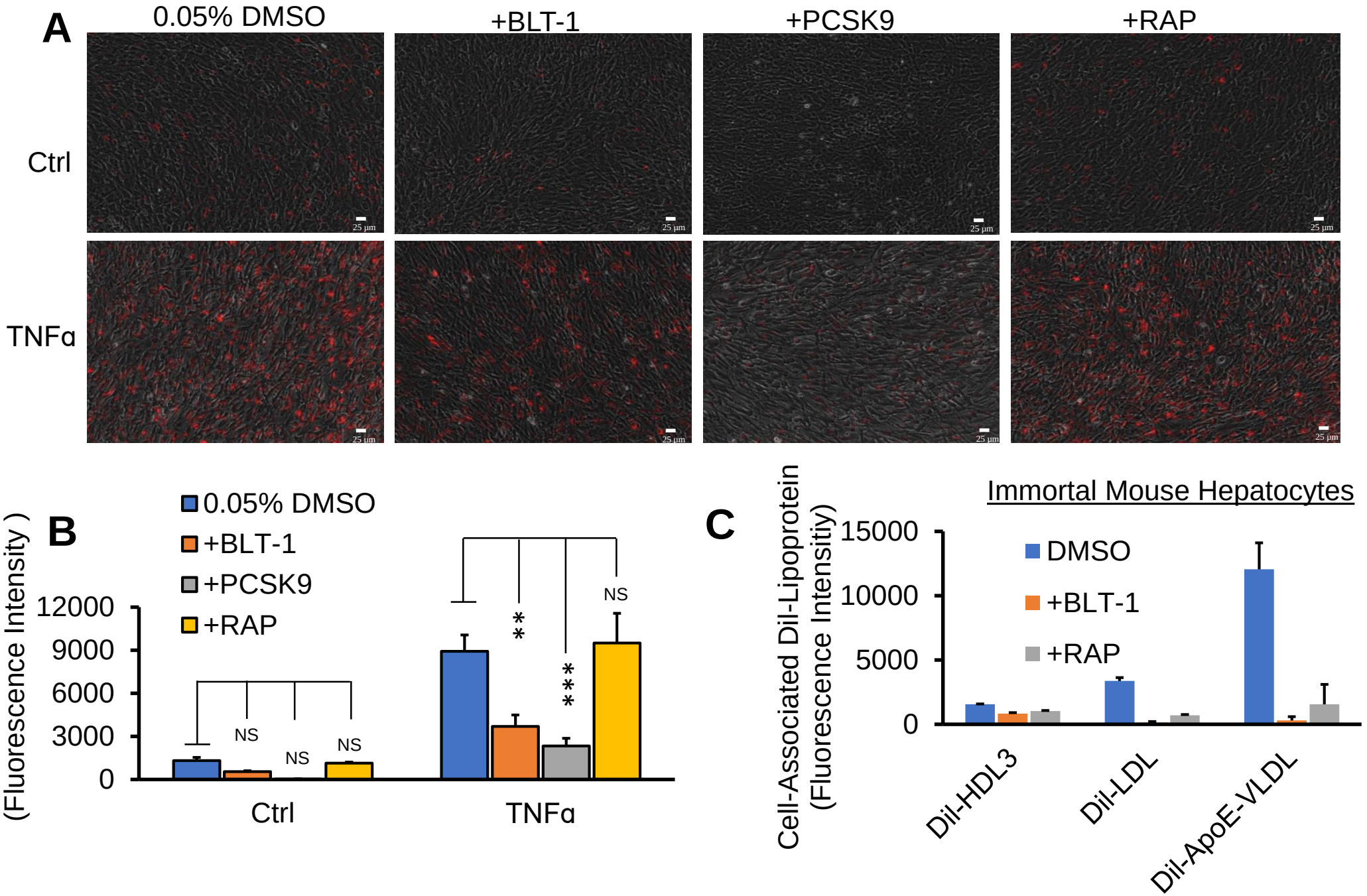
A
0.05% DMSO
+BLT-1
+PCSK9
+RAP
Ctrl
TNFα
25 µm
B
0.05% DMSO
+BLT-1
+PCSK9
+RAP
Cell-Associated DiI-LDL
(Fluorescence Intensity)
12000
9000
6000
3000
0
NS
NS
NS
**
***
NS
Ctrl
TNFα
C
Immortal Mouse Hepatocytes
Cell-Associated DiI-Lipoprotein
(Fluorescence Intensity)
15000
10000
5000
0
DMSO
+BLT-1
+RAP
DiI-HDL3
DiI-LDL
DiI-ApoE-VLDL

Figure 5

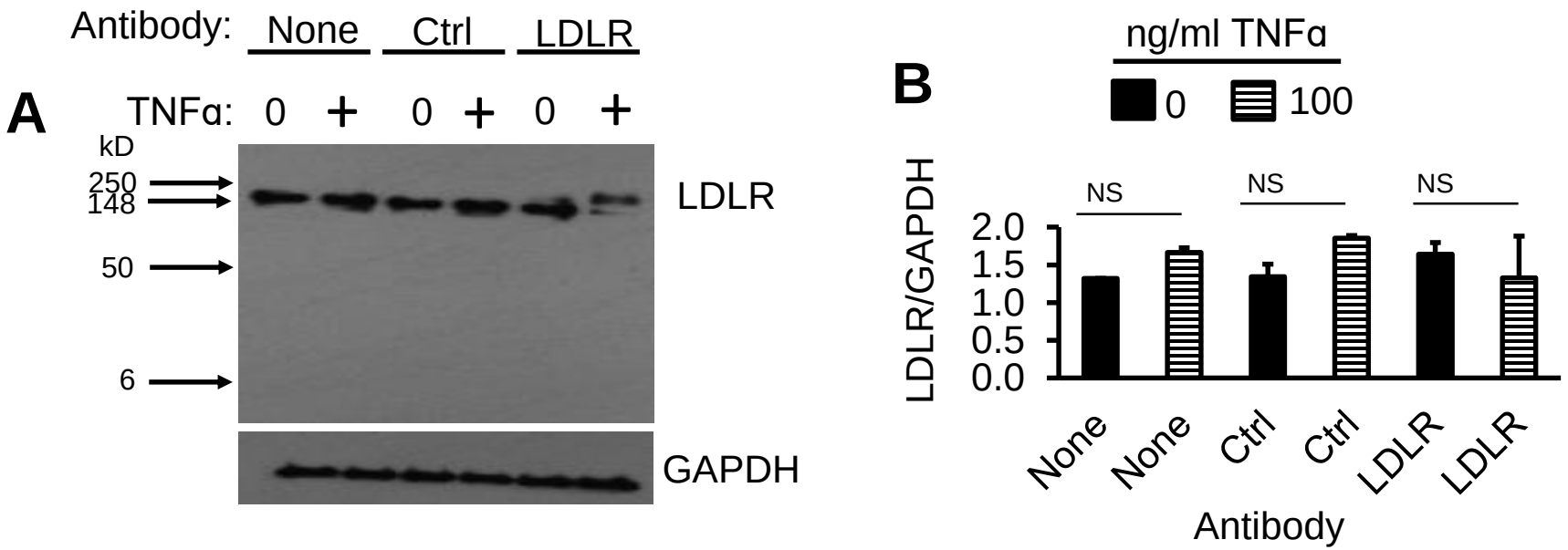
A
Antibody:
None
Ctrl
LDLR
TNFα:
0
+
0
+
0
+
kD
250
148
50
6
LDLR
GAPDH
B
ng/ml TNFα
0
100
LDLR/GAPDH
NS
NS
NS
2.0
1.5
1.0
0.5
0.0
None
None
Ctrl
Ctrl
LDLR
LDLR
Antibody

Figure 6

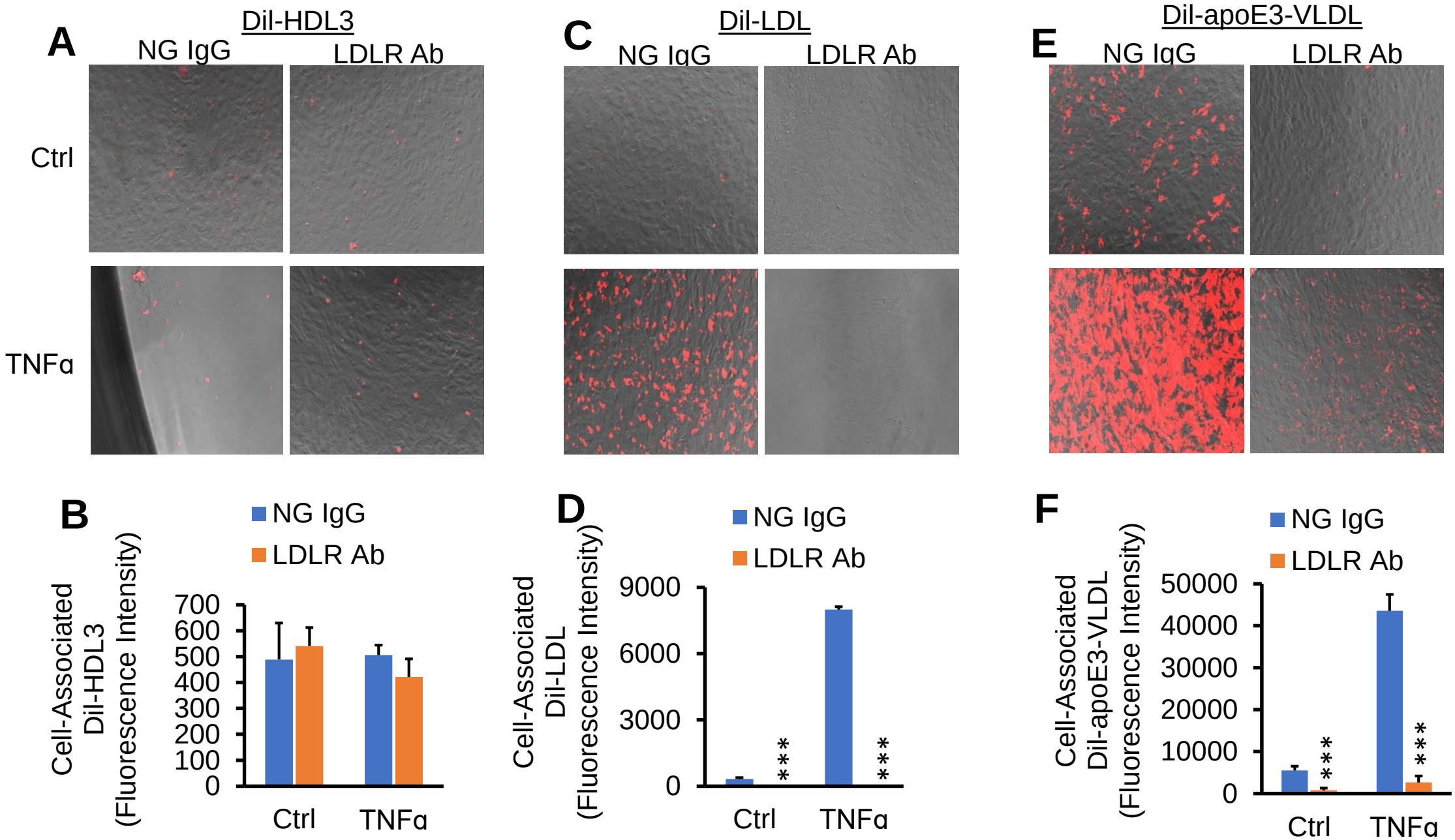
A
Dil-HDL3
NG IgG
LDLR Ab
Ctrl
TNFα
C
Dil-LDL
NG IgG
LDLR Ab
E
Dil-apoE3-VLDL
NG IgG
LDLR Ab
B
NG IgG
LDLR Ab
Cell-Associated Dil-HDL3 (Fluorescence Intensity)
700
600
500
400
300
200
100
0
Ctrl
TNFα
D
NG IgG
LDLR Ab
Cell-Associated Dil-LDL (Fluorescence Intensity)
9000
6000
3000
0
***
***
Ctrl
TNFα
F
NG IgG
LDLR Ab
Cell-Associated Dil-apoE3-VLDL (Fluorescence Intensity)
50000
40000
30000
20000
10000
0
***
***
Ctrl
TNFα

Figure 7

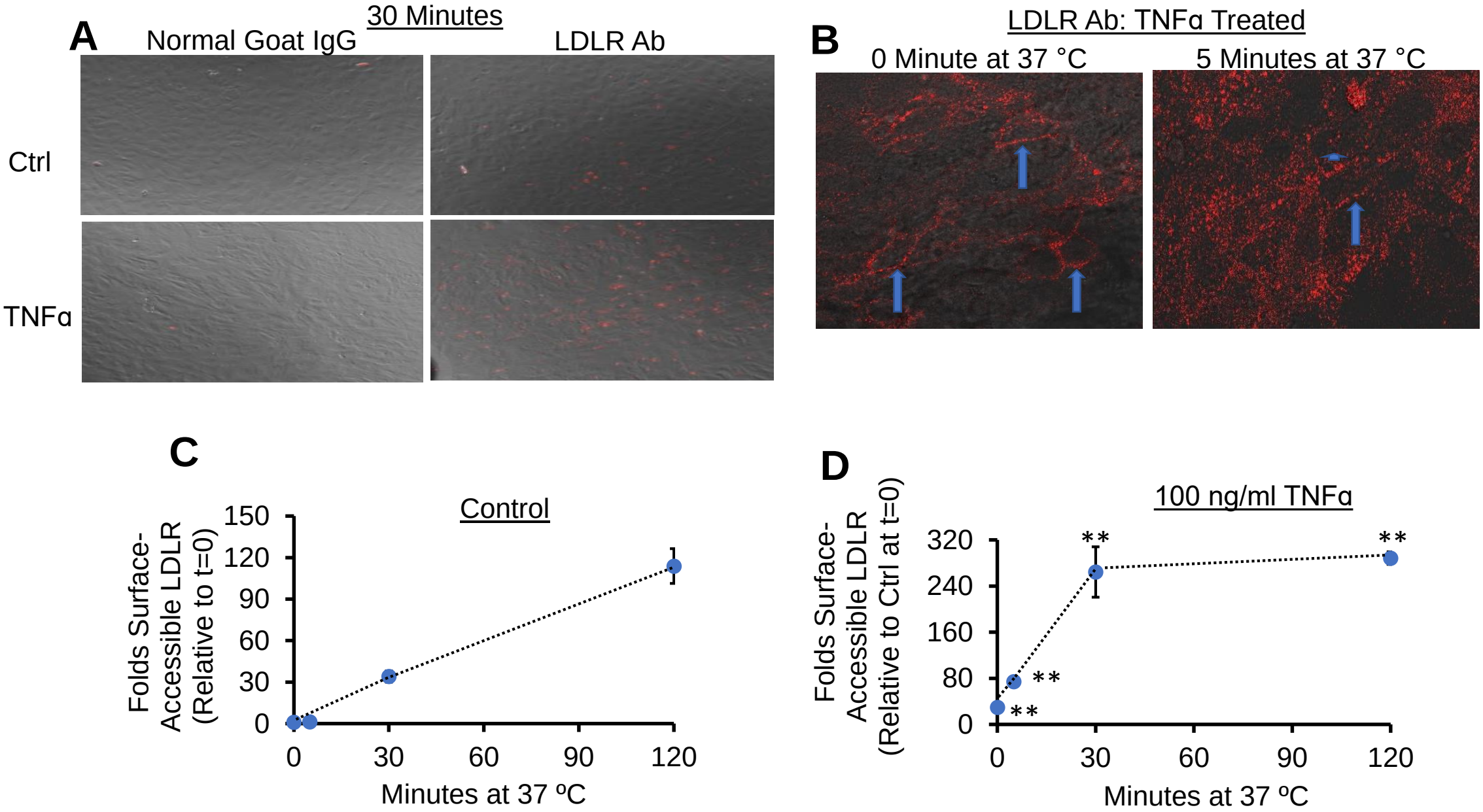
A
30 Minutes
Normal Goat IgG
LDLR Ab
Ctrl
TNFα
B
LDLR Ab: TNFα Treated
0 Minute at 37 °C
5 Minutes at 37 °C
C
Control
Folds Surface-Accessible LDLR (Relative to t=0)
150
120
90
60
30
0
0
30
60
90
120
Minutes at 37 ºC
D
100 ng/ml TNFα
Folds Surface-Accessible LDLR (Relative to Ctrl at t=0)
320
240
160
80
0
**
**
**
0
30
60
90
120
Minutes at 37 ºC

Figure 8

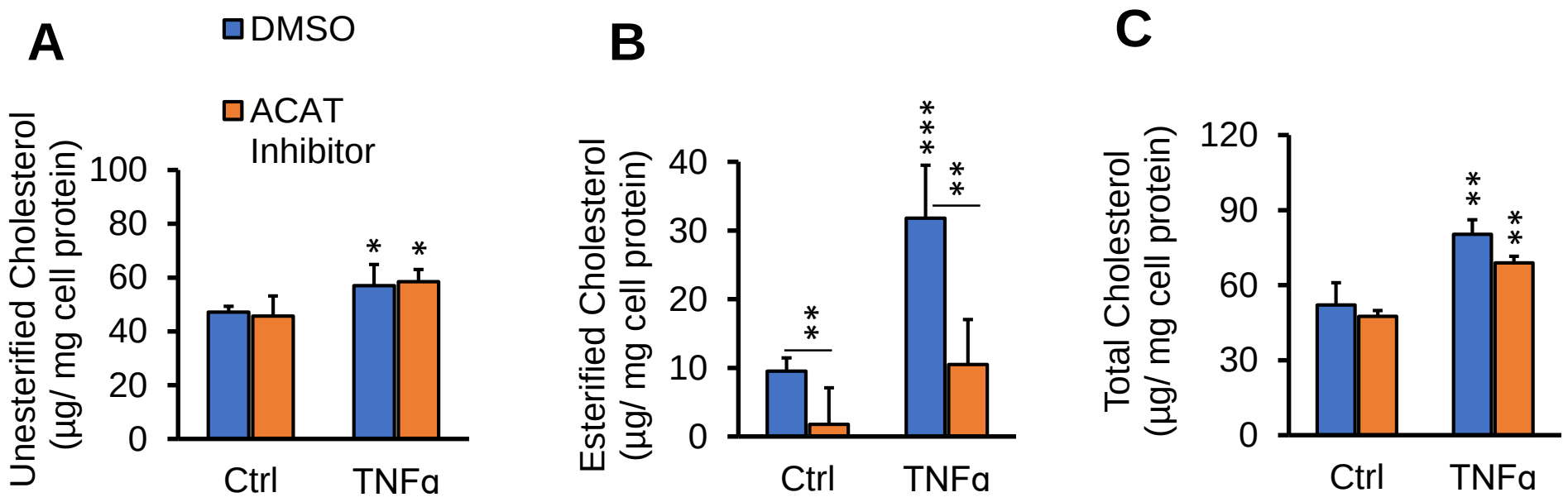
A
DMSO
ACAT Inhibitor
Unesterified Cholesterol (µg/ mg cell protein)
100
80
60
40
20
0
*
*
Ctrl
TNFα
B
Esterified Cholesterol (µg/ mg cell protein)
40
30
20
10
0
**
***
**
Ctrl
TNFα
C
Total Cholesterol (µg/ mg cell protein)
120
90
60
30
0
**
**
Ctrl
TNFα

Figure 9

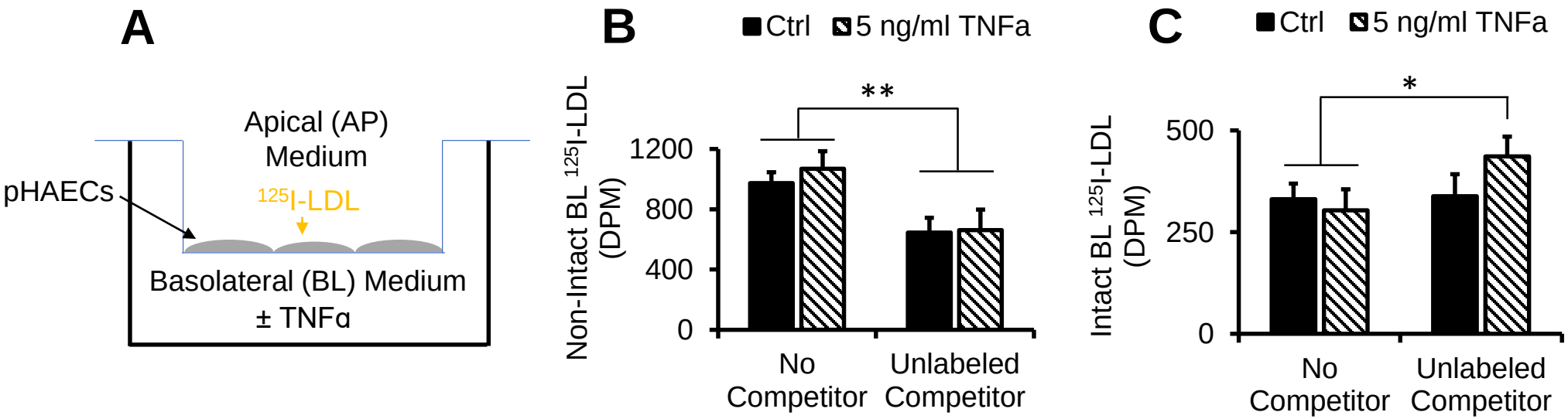
A
Apical (AP)
Medium
pHAECs
125I-LDL
Basolateral (BL) Medium
± TNFα
B
Ctrl
5 ng/ml TNFa
**
Non-Intact BL 125I-LDL
(DPM)
1200
800
400
0
No
Competitor
Unlabeled
Competitor
C
Ctrl
5 ng/ml TNFa
*
Intact BL 125I-LDL
(DPM)
500
250
0
No
Competitor
Unlabeled
Competitor

Figure 10

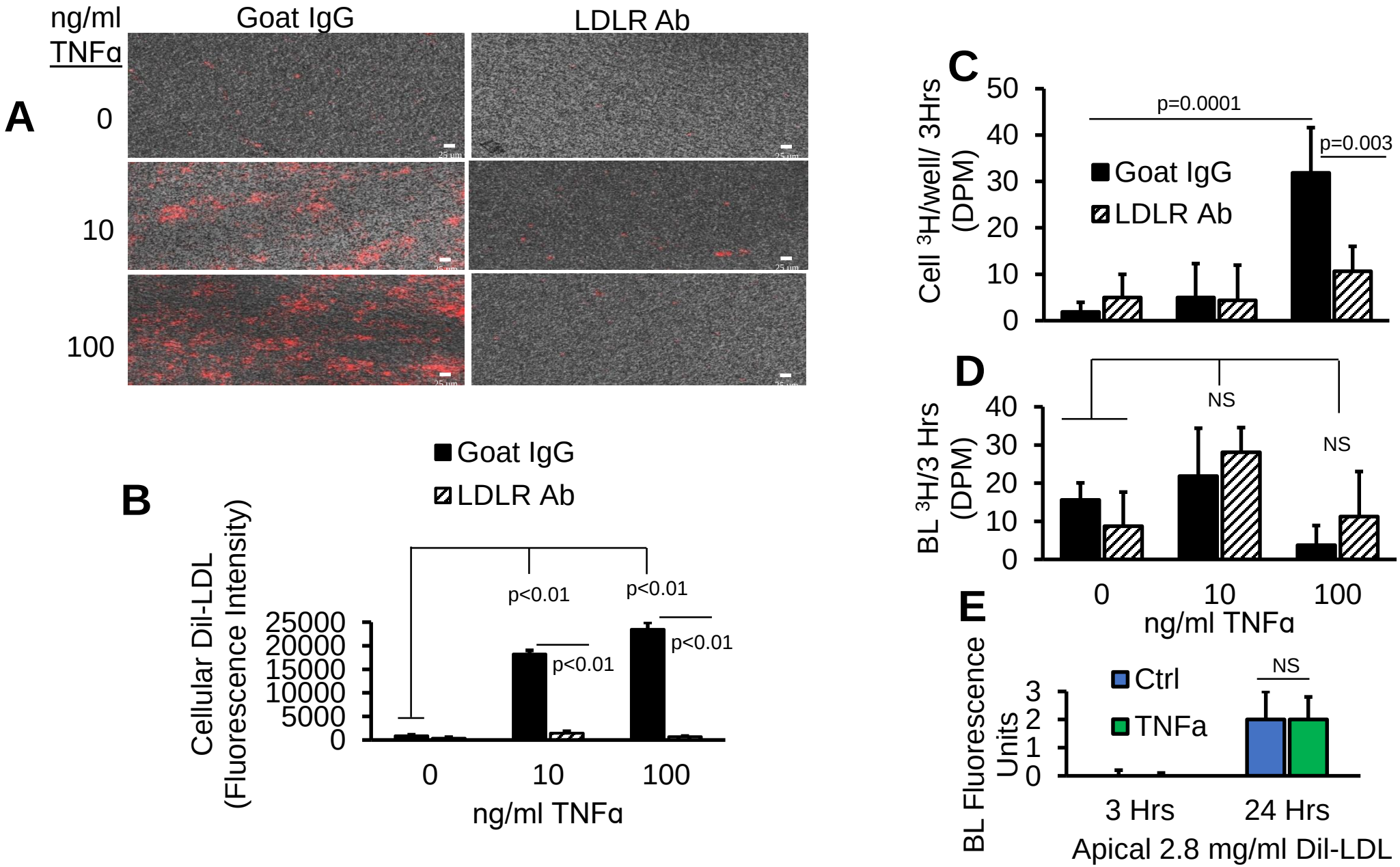
A
ng/ml
TNFα
Goat IgG
LDLR Ab
0
10
100
B
Goat IgG
LDLR Ab
Cellular Dil-LDL
(Fluorescence Intensity)
25000
20000
15000
10000
5000
0
p<0.01
p<0.01
p<0.01
p<0.01
0
10
100
ng/ml TNFα
C
Cell ³H/well/ 3Hrs
(DPM)
50
40
30
20
10
0
p=0.0001
p=0.003
Goat IgG
LDLR Ab
D
BL ³H/3 Hrs
(DPM)
40
30
20
10
0
NS
NS
0
10
100
ng/ml TNFα
E
BL Fluorescence
Units
3
2
1
0
Ctrl
TNFa
NS
3 Hrs
24 Hrs
Apical 2.8 mg/ml Dil-LDL

Figure 11